Communications Research Centre Canada
An Agency of Industry Canada

Centre de recherches sur les communications Canada
Un organisme d'Industrie Canada

Angular filter study to modify the beam of a high gain antenna (Phase 1)

Jafar Shaker

CRC Technical Note no: CRC-TN-2006-001

September 2006

CRC

Angular Filter Study to Modify the Main Beam of a High Gain Antenna (Phase I)

Jafar Shaker

Abstract

Development of techniques to suppress radiation into regions close to the main lobe of a high gain antenna is the subject of this report. A cascade of Frequency Selective Surfaces (FSS's) was used as the building blocks of a 3rd order Chebishev filter as an angular filter that operates within the frequency band of the filter. Necessary theoretical development was undertaken to establish parallels between electromagnetic characteristics of an FSS and circuit parameters that are used in the realization of Chebishev frequency response. Experimental methods were devised to characterize the phase response of an FSS structure. Knowledge of the phase response of each individual layer proves to be critical in the overall design process of the Chebishev filter. Insight gained during the characterization of the filter was essential in the rather "gradual" process of the design and fabrication of test apparatus. This insight leads to guidelines about the tolerances and critical parameters in the design and operation of such cascade filters.

Introduction

The congestion of earth orbits with satellites that provide different multimedia communications services within the same frequency band has rendered indispensable the study of methods to mitigate the interference between different satellites at the RX side. The angular separation between the satellites can be so close at times that currently operational systems might not be able to suppress interference between their corresponding satellite and newly lunched satellites that are in its close proximity. It is obvious that the antenna system can be replaced in order to meet new specifications. However, it is preferred to implement add-on systems to avoid the cost of redesigning new systems. The subject of this report is development of design, fabrication, and test guidelines for a cascade of FSS's as the building blocks of a Chebishev filter that is to be placed onto the aperture of a radiating system in order to alter its radiation characteristics in compliance with new specifications different from the ones that were originally used in the design of the radiating system.

The first section of the report deals with the possibility of using a single layer FSS as the add-on structure to modify the radiating characteristics of an existing antenna system. Parallels between the circuit parameters of a Chebishev filter and field characteristics of an FSS will be drawn and discussed in the second section of the report. Characterization of the phase response of an FSS is the subject of the subsequent section. Fourth section of the report deals with two methods for the characterization of a Fabry-Perot resonator that is composed of two layers of FSS structures. The first method is direct measurement of the resonator whereas in the second method, measurement of each single layer in conjunction with an in-house developed code was used to characterize the Fabry-Perot resonator. Having obtained specifications of a Chebishev filter given design specifications in section 5, High Frequency Simulation Software (HFSS) was used to verify the realization of the Chebishev filter which agreed well with another numerical method that was proved to be much faster and used HFSS simulation of single layer in conjunction with an in-house developed computer code. The test apparatus and the experimental data for the cascade of FSS's will be shown in the subsequent section. Also, the angular sensitivity of the filter will be briefly discussed in the same section. The last

section of the report includes recommendation for further research and concluding remarks.

1- Single layer and double layer FSS

The possibility of utilization of single or double layer FSS structure will be assessed in this section. The theoretical framework is presented and used to characterize conventional FSS structures.

1-1. Brief description of the method of analysis

Method of moment (MoM) was used to find the current distribution on the constituent cell elements of the periodic structure. Knowing the current distribution, the reflective characteristics of a periodic structure can be calculated. In this section the MoM formulation for a periodic structure composed of conducting patches of irregular shape is described briefly. The formulation can be generalized to encompass the periodic perforated screen composed of irregular openings. The formulation and its numerical aspects have been thoroughly presented in [1].

The imposition of boundary condition on the constituent element of a periodic structure leads to the following integral,

$$\vec{E}_{inc}(x,y,0) = \frac{-1}{T_x T_y} \int_S \ddot{G}(x,y,0 \mid x',y',0).\vec{J}(x',y')dx'dy' \qquad (1)$$

where $T_{x(y)}$ is the cell dimension in the $x(y)$ direction, $\ddot{G}(x,y,0 \mid x',y',0)$ is the dyadic Green's function of the structure for which both the source $(x',y',0)$ and observation points $(x,y,0)$ are located on the patch, and $\vec{J}(x',y')$ is the unknown current distribution on the patch. It should be noted that the dyadic Green's function for a two-dimensional periodic structure is a double summation of Floquet's modes given as follows,

$$\ddot{G}(x,y,z \mid x',y',0) = \frac{1}{T_x T_y} \sum_m \sum_n \ddot{g}^{(E)}(k_{xm},k_{yn}) e^{j(k_{xm}(x-x')+k_{yn}(y-y'))} e^{jk_{zmn}z} \qquad (2)$$

where $\ddot{g}^{(E)}(k_{xm},k_{yn})$ is the Green's function of the E-field in the spectral domain, and k_{xm}, k_{yn}, and k_{zmn} are given as,

$$k_{xm} = k_0 \sin\theta_{inc} \cos\phi_{inc} + \frac{2\pi m}{T_x} \qquad k_{yn} = k_0 \sin\theta_{inc} \sin\phi_{inc} + \frac{2\pi n}{T_y}$$

$$k_{zmn} = \sqrt{k_0^2 - k_{xm}^2 - k_{yn}^2} \tag{3}$$

Note that "θ_{inc}" and "ϕ_{inc}" designate the direction of the incident plane wave. Using triangular basis functions as the test and basis functions to discretize (1) which is an integral equation, the following set of linear equations is obtained,

$$\begin{bmatrix} Z_{xx} & Z_{xy} \\ Z_{yx} & Z_{yy} \end{bmatrix} \begin{bmatrix} I_x \\ I_y \end{bmatrix} = \begin{bmatrix} V_x \\ V_y \end{bmatrix} \tag{4}$$

Each of the elements of the square matrix is a submatrice whose elements describe the reaction integral between source and test functions. A commonly used matrix inversion algorithm, namely, LU decomposition was used to find the unknown current distribution on the cell element.

1-2. Single layer FSS structures

Fig. 1 shows the side and top views of a single layer FSS structure which is composed of a lattice of conductors etched on a single dielectric slab. In the resonant conditions, the surface emulates a reflective surface. Fig. 2 shows the simulation results for an FSS composed of patches that are etched on a dielectric slab and is resonant in the X-band. An extensive set of simulations was carried out to investigate the angular sensitivity of the structure around the resonance frequency and the result is shown in Fig. 3. The filter can be operated in the dip region of the respective angular plot. As can be seen the reflected power is minimum in the dip region of the graph shown in Fig. 3. Therefore, tilting the filter by 2^o when it operates at 11.8 GHz, would result in very low insertion loss for the main beam and a high reflection along 2^o (which was broadside direction prior to the rotation of the filter). However, it should be noted that the dip shifts as the operating frequency changes. This seems to be a general rule for single layer FSS structures which was confirmed through numerous and extensive simulations for which the aspect ratio of the patches, dielectric constant of the substrate and its thickness, and the lattice size were varied. This led to the rejection of single FSS layer for the present application because of its extreme sensitivity to variation of the operating freqeuncy.

1-3. Two layer FSS structures

A similar exercise as in the last section was carried out for structures that are built by cascading two FSS structures. Fig. 4 shows the side and top views of such structures. The cell elements on the top and bottom layers are patches. Fig. 5 shows the simulation result for the frequency response of a typical two layers FSS structure. The multi resonant behaviour is due to the presence of two resonant structures. Again, simulations were performed to obtain the angular sensitivity of the structure for different frequencies and the results are shown in Figs. 6. As in the of single layer FSS structures, the "reflection valley" shifts as the operating frequency is varied. It should be noted that a large variety of two layers FSS structures were simulated for different combination of parameters such as: patch size, lattice size, dielectric constant of the substrate, and its thickness. However, the general trend of moving "reflection valley" persisted for different sets of design parameters.

1-4. Perforated screens

A perforated screen is composed of a periodic lattice of apertures in a conductor that is etched on a dielectric slab. Such structures represent low insertion loss at resonant. The side and top views of a typical perforated screen with rectangular apertures is shown in Fig. 7. The frequency response of a typical perforated screen is shown in Fig. 8. Perforated screens were deemed to be suitable for the suppression of unwanted radiation as they have low insertion loss in resonance and have sharp angular response. However, as shown in Figs. 9 their angular response shifts as the frequency varies. Therefore, perforated screens suffer from the same shortcoming that was described in the last two sections.

2. Cascade of Frequency Selective Surfaces to emulate Chebishev filters

A cascade of frequency selective surfaces has been suggested in the literature [2] in order to realize a prescribed frequency response. The filters are 1-D periodic structure of conducting metallic strips. A relationship is found between the circuit parameters of the desired filter and the structural parameters of the FSS such as: the strip width, periodicity,

substrate thickness, *etc.* Having thus obtained the structural parameters to attain the required frequency bandwidth, the whole structure can be tilted in order to achieve the prescribed angular response.

2. The relationship between circuit parameter and field parameters

The block diagram that is generally used in the conventional design of microwave filters is shown in Fig. 10. By adjusting the inversion ratios of each stage, "*K*", and also the resonant length of the connecting stage between the consecutive inverter block, "*L*", different types of filters can be synthesized as has been extensively described in [3] and [4]. An FSS implementation of such a block diagram is shown in Fig. 11. There is a relationship between the inversion parameter of a particular stage shown in Fig. 10 and its "S_{11}" performance as shown in Fig. 12. The method suggested in [3] was used for the circuit analysis. The design algorithm for an "*N*th" order low pass Chebishev filter of a given ripple "*k*" can be briefly described as follows:

Given the bandwidth and passband ripple of the desired Chebishev Low Pass Filter (LPF), element values can be derived from the following relation,

$$R = \begin{cases} 1 & N\ odd \\ 2k^2 + 1 - 2k\sqrt{1+k^2} & N\ even \end{cases} \tag{5}$$

and where "*k*" represents the ripple. The values of inductance (in Henry) and capacitance (in Farad), "g_k", of the LPF shown in Fig. 13 can be calculated using the following relationship:

$$g_k = \frac{4a_{k-1}a_k}{b_{k-1}g_{k-1}} \tag{6}$$

where

$$a_k = \begin{cases} 0.5 & k = 0 \\ \sin\dfrac{2k-1}{2N}\pi & k = 1,2,\cdots \end{cases} \tag{7}$$

$$b_k = \begin{cases} \sinh\dfrac{\beta}{2N} & k = 0 \\ \sinh^2\dfrac{\beta}{2N} + \sin^2\dfrac{k\pi}{N} & k = 1,2,\cdots \end{cases} \tag{8}$$

$$\beta = \ln\frac{\sqrt{1+k^2}-1}{\sqrt{1+k^2}+1} \tag{9}$$

Knowing the values of the circuit components, the input impedance, Z_{in}, can be calculated that leads to the following expression for the reflection coefficient of the whole circuit:

$$\Gamma = \frac{Z_{in}-1}{Z_{in}+1} \tag{10}$$

A low-pass filter can be transformed into a high-pass, band-pass, and other types of filters by appropriate frequency transformations. Therefore, to design a filter other than low-pass filter, its low-pass equivalent is derived first and then the desired filter can be obtained by using transformation formulas.

The transformation of low-pass to band-pass filter leads to a circuit realization that includes both parallel and series resonant circuits. Impedance inverter circuits are used as a means of circuit realization that solely consist of either series or parallel resonators as shown in Fig. 14. The inversion parameters of the filter can be derived from the circuit parameters by using the following relationship:

$$K_{k,k-1} = \begin{cases} \sqrt{\dfrac{L_{0k}L_{0k-1}}{L'_k C'_{k-1}}} & k \text{ even} \\ \sqrt{\dfrac{L_{0k}L_{0k-1}}{C'_k L'_{k-1}}} & k \text{ odd} \end{cases} \tag{11}$$

Detailed formulas and derivation of circuit parameters in the above equation can be found in [3]. Circuit parameters of the many circuit realizations of the impedance inverter can be fully determined after calculation of "*K*" in equation (11). One such circuit realization

comprised of a transmission line and a shunt impedance [4] is shown in Fig. 15. The circuit parameters are given in the following:

$$K = Z_0 \tan\left|\frac{\phi}{2}\right| \tag{12}$$

$$\phi = -\tan^{-1}\frac{2X}{Z_0} \tag{13}$$

$$\left|\frac{X}{Z_0}\right| = \frac{\frac{K}{Z_0}}{1-\left(\frac{K}{Z_0}\right)^2} \tag{14}$$

Determination of the "Γ_{in}" of each impedance inverter in isolation of the other filter stages defines the reflective characteristic that is to be emulated by the corresponding FSS. Fig. 12 is a representation of the correspondence between these two parameters.

The following procedure was developed and followed during the course of this project to synthesize 3rd order Chebishev filter in order to attain a given frequency response:

1- Given the operating frequency, frequency bandwidth, and ripple the circuit parameters of the Chebishev filter were determined.
2- Impedance inversion parameters of the filter are found.
3- The reflection coefficient of each of the impedance inverter circuits is found.
4- The structural parameters of the strip grating FSS are varied until the reflection coefficient of the previous step is realized.

The periodicity of the strip grating was chosen to ensure significant decay of higher order Floquet modes of each constituent layer before reaching the adjacent FSS layers. Practical consideration such as mechanical robustness and cost were used to choose the dielectric substrate.

The angular sensitivity of the filter can be modified by rotating its constituent stages [2]. Therefore, in the event of the deviation of the angular sensitivity of filter that is designed

using the above four step algorithm from desired specifications, the whole process can be repeated as all the constituent stages are rotated by a constant angle "θ". The process should be repeated until the desired angular sensitivity is achieved.

Initially, the frequency response of each constituent stage was obtained using the circuit analysis. Having set the order of Chebishev filter to 3, four stages were required to synthesize the filter while the mirror symmetry of the filter around its mid-plane reduces the unknowns by a factor of two. Figure 16 shows the frequency response of the first two stages. Then, the impact of the variation of the strip width of a strip grating was studied using full wave software tool in order to find the best match between the reflective characteristics of the strip grating and the particular filter stage that it was to emulate. Fig. 17 shows a view of the filter and also a typical graph that shows the effect of strip-width on the reflective characteristics of the individual FSS layer.

Having designed equivalent FSS layers using a full wave software tool such as Picasso and HFSS and knowing the frequency response of each constituent stage of the cascaded filter, the frequency response of the whole structure can be calculated by either time consuming full wave softwares or fast and robust circuit analysis software based on the above guidelines. To verify the agreement between the circuit method and full-wave softwares, gradual evolution of the filter composed of FSS layers is shown in Figs. 18-20.

3. Measurement

Strip gratings with different strip-width were fabricated and measured to observe the effect this parameter on the frequency response of the FSS. The measured results in Fig. 21 can be used to establish an empirical relationship between the strip-width and inversion parameter of the FSS. This knowledge can be used in selecting structural parameters of FSS in order to realize the desired frequency response.

Fig. 22 shows the measurement apparatus which is a quasi-optical measurement system that has been described in detail in [5]. Also shown in the same figure is the four stage Chebishev filter composed of FSS layers.

To verify the validity of the circuit-based computer code, Fabry-Perot resonators composed of two similar FSS layers were built by embedding a foam spacer between them as shown in Fig. 23. The "measured" scattering parameters of a single layer FSS were then used as the input of the cascade routine to obtain the reflective characteristics of a cascade of two FSS layers. The result is in good agreement with the measurements as shown in Fig. 24. It is interesting to note that the software is capable of predicting the shift of the resonance frequency as a result of changing the separation between the two FSS layers. A representation of the high sensitivity of frequency response of cascade structure on separation between layers is shown in Fig. 25 where cascade routine has been used. It can be observed that a change of 0.1 mm in the separation between layers 2 and 3 has significantly modified the frequency response of the whole assembly. This phenomenon was further verified by using HFSS that is a full package and the result is shown in Fig. 26. Metallic shims were used in addition to foam separators to maintain the separation between two adjacent layers.

A novel measurement procedure was developed to measure rather unequal phase response of "S_{11}" and "S_{22}" of each FSS layer that is the result of innate difference between the sides of the FSS [6]. Knowledge of phase response of the scattering parameters of the isolated FSS is necessary if they are to be used in the calculation of cascade filter. The method has been described in detail in [6].

The initial plan was to use isolated measurement of each constituent layer as the input for the cascade routine to find the optimum separation between the filters that result in the desired frequency response and avoid running very time consuming full wave softwares. However, extreme sensitivity of cascade response to any minor change in the separation between the two layers and non-repeatability of experiments because of the softness and fragile nature of the foam separators limited the applicability of the cascade routine significantly.

In absence of a reliable software tool and fabrication related uncertainties such as spacer thickness and its flatness, empirical optimisation of the separation between the layers of the constituent stages of the filter was resorted to realize the filter desired response. Consecutive stages of the filter were introduced one by one and the separation between each layer that was added to the assembly and its adjacent already present layer was changed until the corresponding frequency response of Figs. 18-20 was approximated as close as possible. This method has been demonstrated in Fig. 27 to find the spacing layers 2 and 3. It is evident that the separation of 4.8mm between these two layers results in the best agreement between the measured three layers response and what is suggested in Fig. 19. The result of this process is shown in Figs. 28 and 29. A summary of the previous figures that shows the frequency response of the optimised filter is shown in Fig. 30 where data smoothing has been used to remove the ripples.

To acquire a better understanding of the impact of separation between layers on the frequency response of the filter, shims were inserted between layers 2 and 3 on only one side (c.f. Fig. 31a) and the results are summarized in Fig. 31b.

4- Recommendation for further research

One of the shortcomings of this research that persisted throughout was prevalent utilization of foam material as a means of maintaining prescribed separation between adjacent layers. Observation of the high sensitivity of filter frequency response to the separation between layers did not come as a surprise when it was recalled that these separations actually define and dictate resonant conditions that are pre-requisites for realization of any higher order filter. Therefore, an obvious recommendation for further research is to avoid using foam as the separating medium and replace with dielectric substrate of the same type that is used in the fabrication of the constituent FSS layers. Such a development calls for minor modifications in the circuit analysis computer code the most import of which is replacing air separator by dielectric substrate of choice.

5- References

1. Jafar Shaker, "Analysis of multiplayer double periodic structures and their performance", Ph.D. Dissertation, Department of Electrical and Computer Engineering, University of Manitoba, 1995.

2. D. Kinowski, M. Guglielmi, and A. Roederer, "Angular Bandpass Filters: An Alternative Viewpoint Gives Improved Design Flexibility", *IEEE Trans. on Antenna and Propagation*, Vol. 43, No. 4, Apr. 1995, pp. 390-395.

3. R. Collin "Foundations for microwave engineering", Mc. Graw-Hill, 1966

4. G. Matthaei, L. Young, and E. M. T. Jones, "Microwave Filters Impedance-hfatching Networks, and Coupling Structures" Denham, MA, Artech House, 1980.

5. Nicolas Gagnon, "Design and study of a free-space quasi-optical measurement system", CRC-Report, No. CRC-RP-2002-02.

6. N. Gagnon, and J. Shaker, "Accurate phase measurement of passive non-reciprocal quasi-optical components", IEE Proceedings of Antennas, Microwave, and Propagation, Vol. 152, No. 2, Apr. 2005, pp. 111-116.

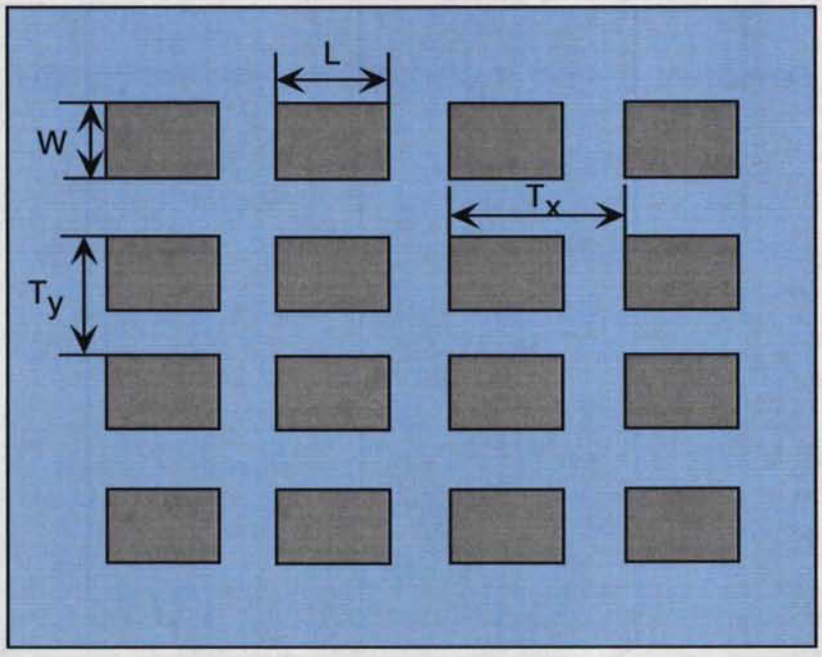

(a)

(a)

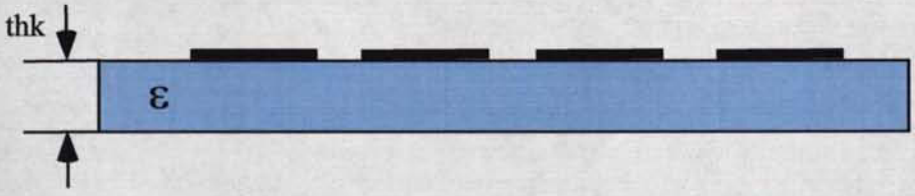

(b)

Fig. 1- Top and side views of a single layer FSS structure: (a) Top view. (b) side view.

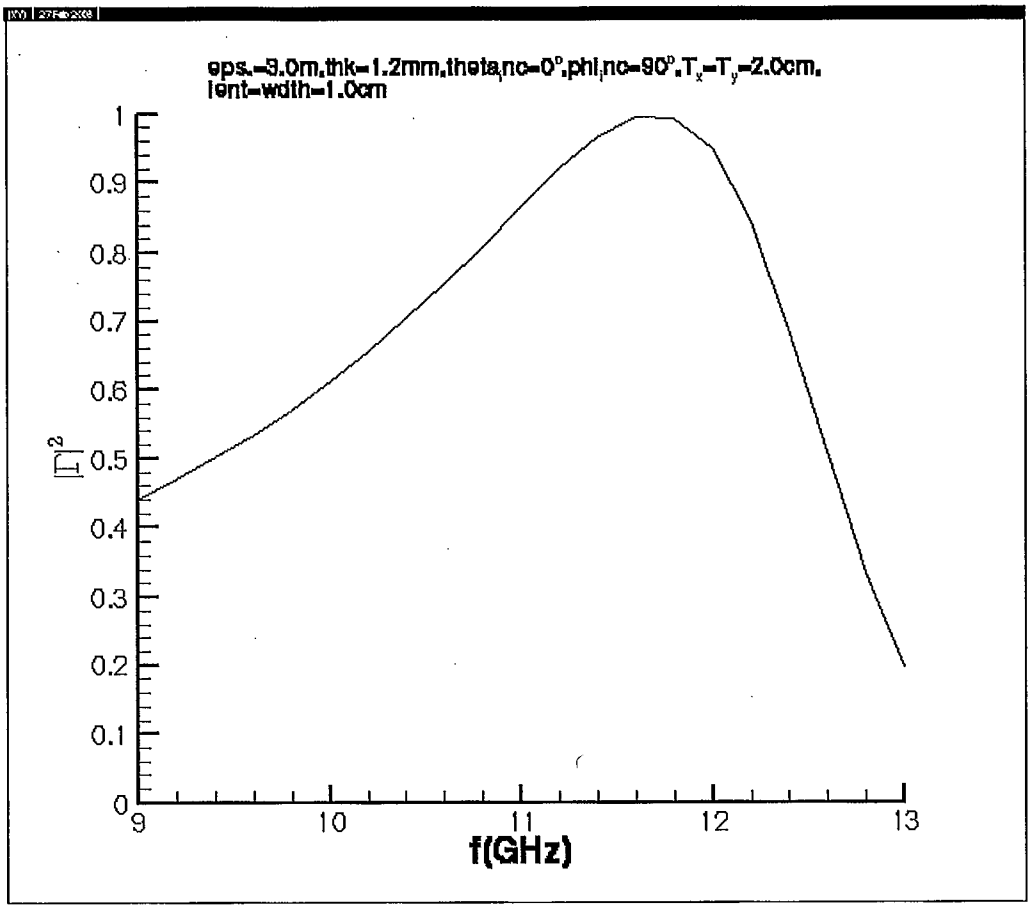

Fig. 2- Frequency response of an FSS illuminated by a normally incident plane wave. The parameters in the graph title have been described in Fig. 1.

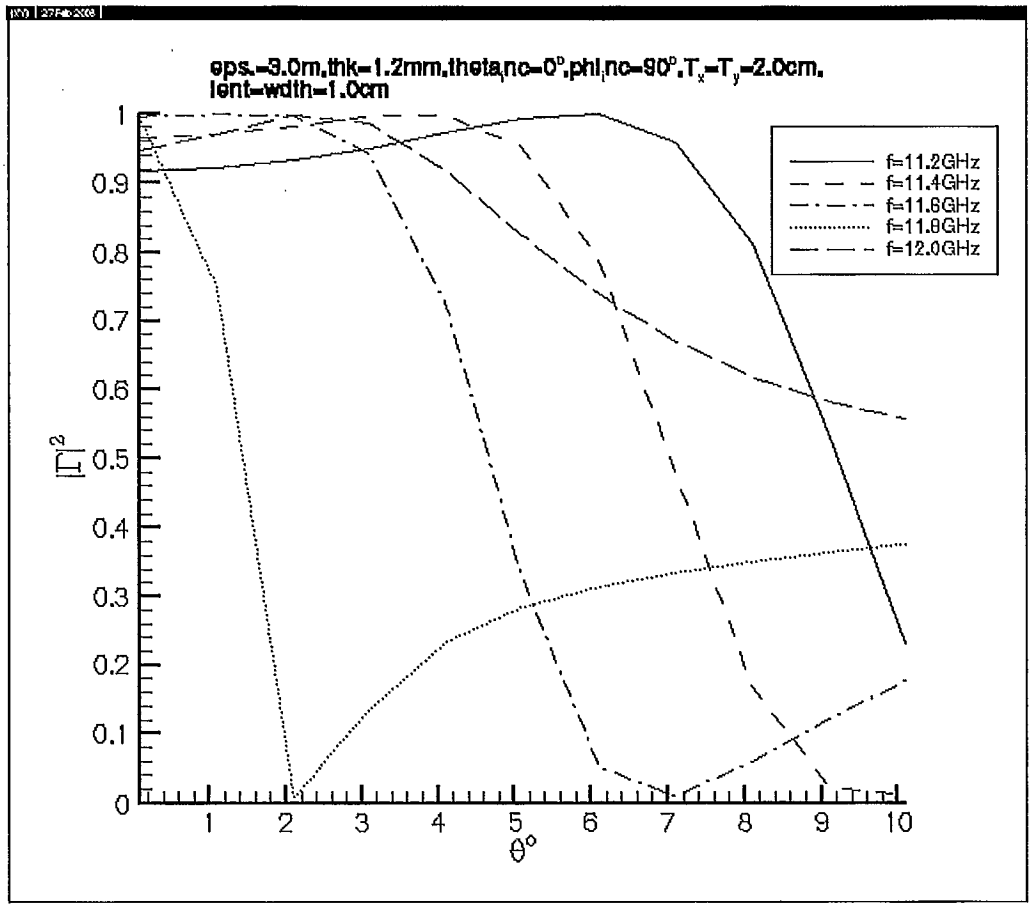

Fig. 3- Angular sensitivity of the FSS at different operating frequencies. The description of the parameters in the title of the graph can be found in Fig. 1.

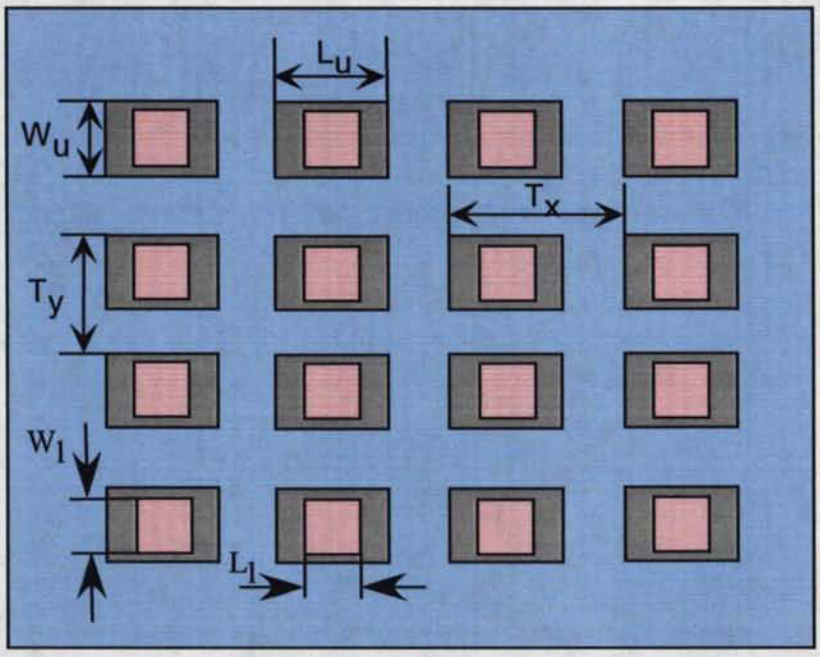

(a)

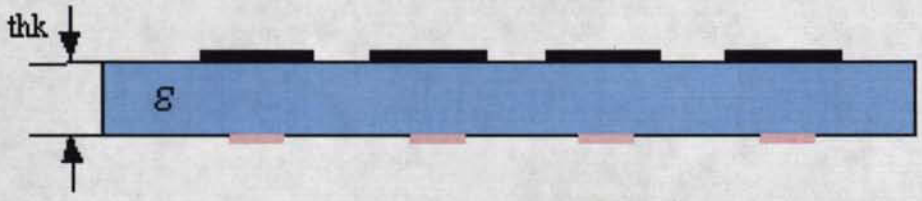

(b)

Fig. 4- Fig. 1- Top and side views of a douple layer FSS structure: (a) Top view. (b) side view.

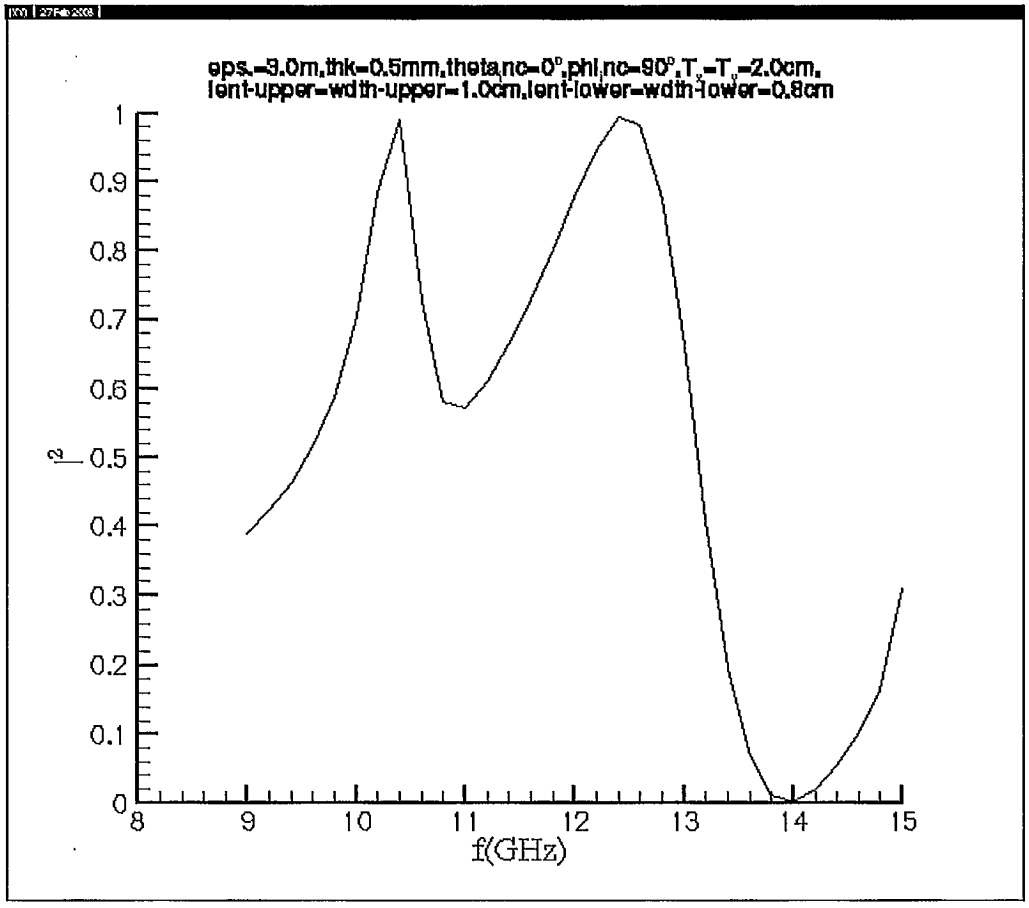

Fig. 5- Frequency response of a periodic structure composed of two FSS layers illuminated by a normally incident plane wave. Parameters in the title of the graph are described in Fig. 4.

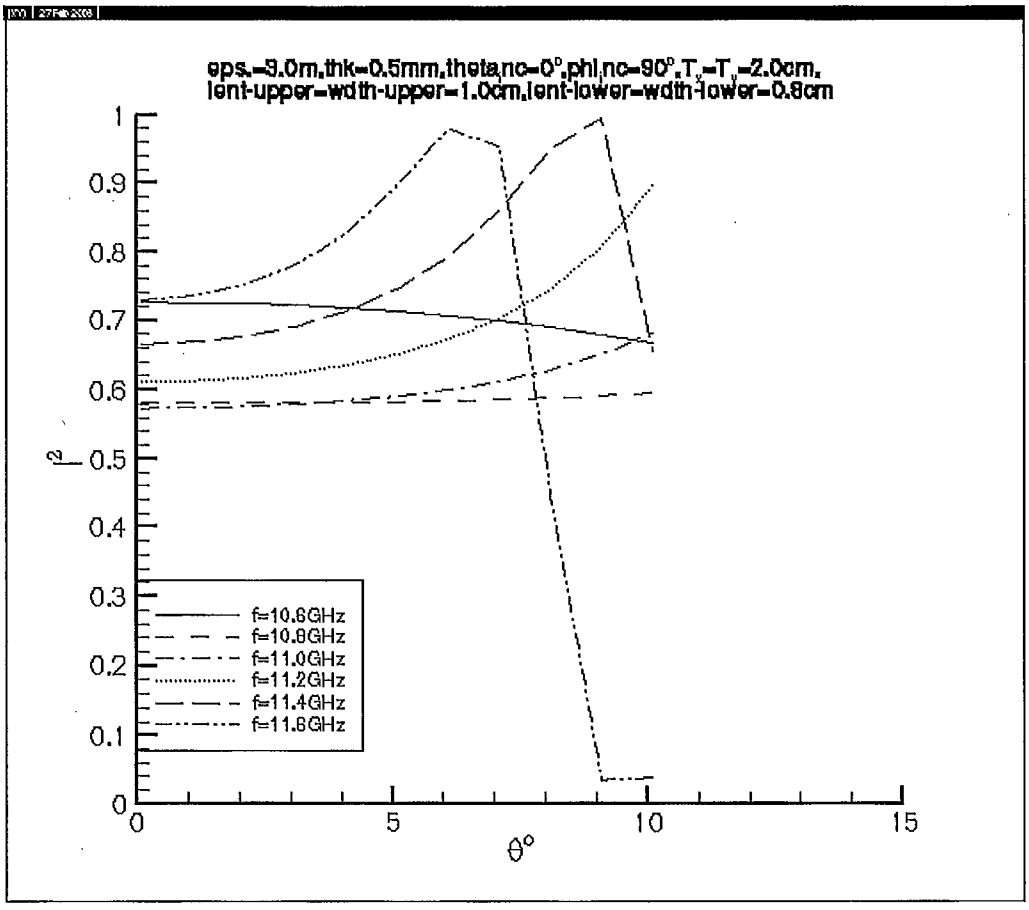

Fig. 6a- Angular sensitivity of a typical two layer FSS structure. The parameters in the title of the plot are described in Fig. 4.

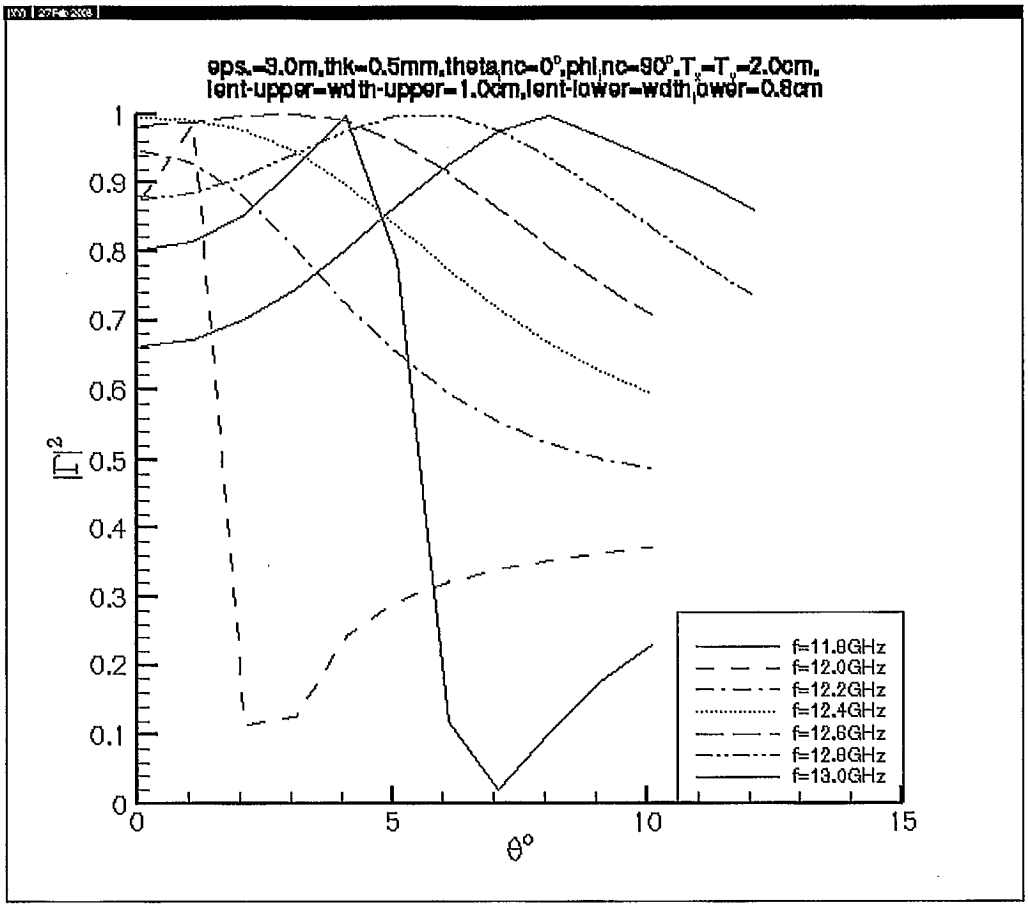

Fig. 6b- Angular sensitivity of a typical two layer FSS structure. The parameters in the title of the plot are described in Fig. 4.

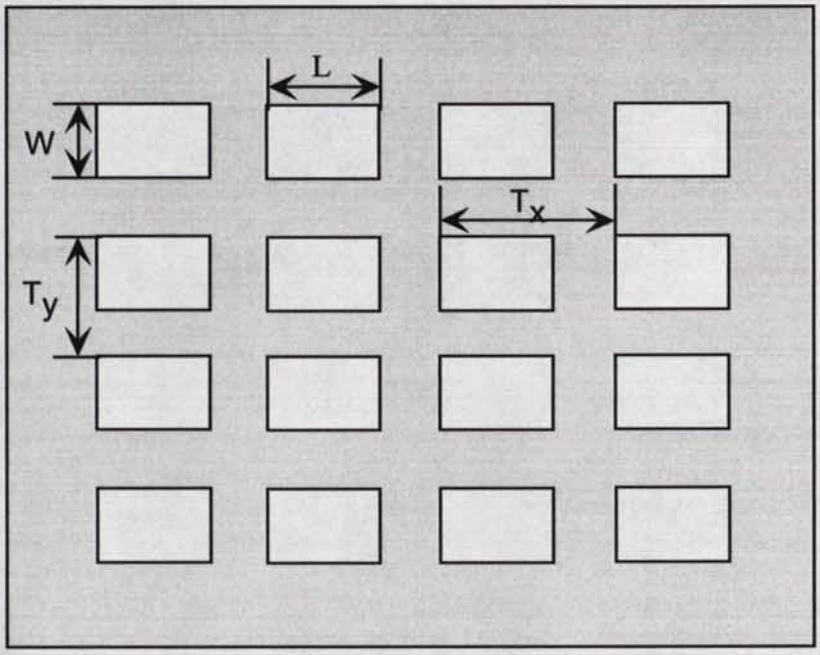

(a)

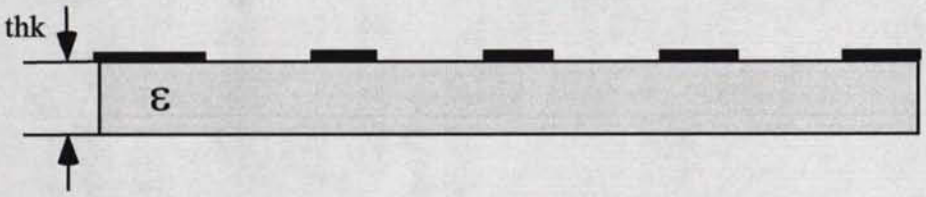

(b)

Fig. 7- Top and side views of a perforated screen: (a) Top view.
(b) Side view.

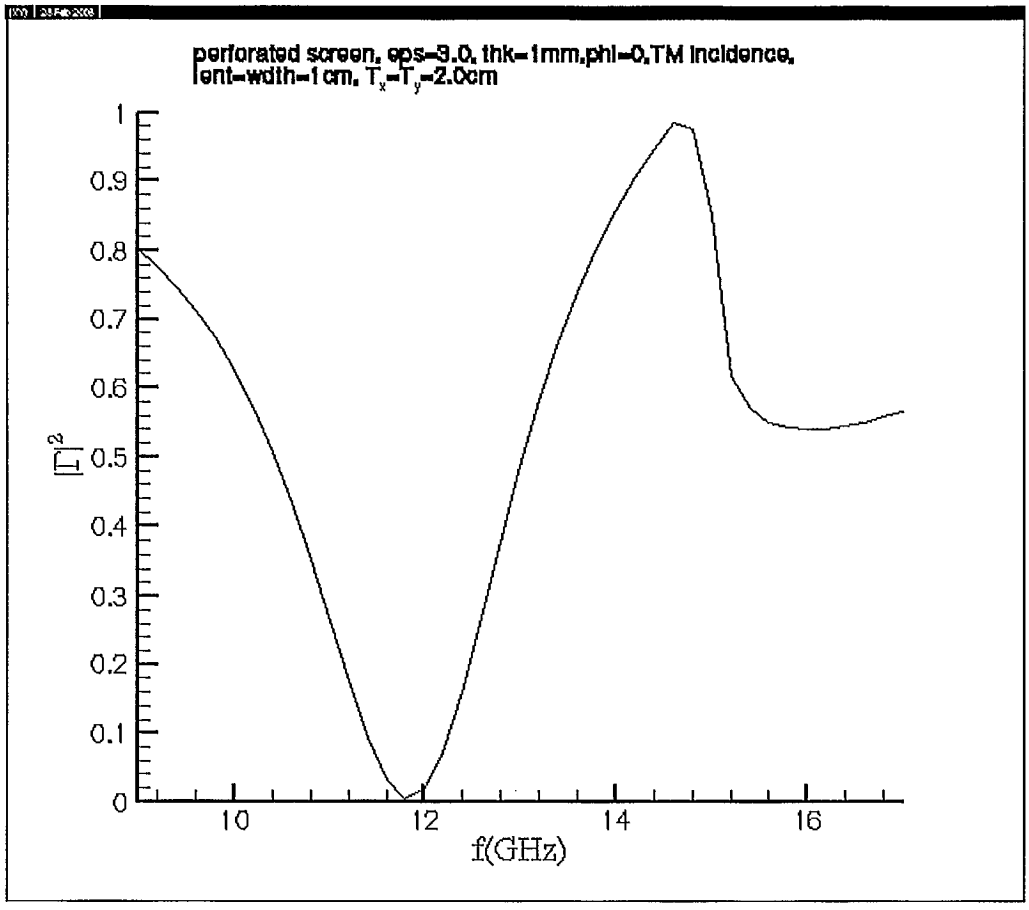

Fig. 8- Frequency response of a periodic structure composed of two FSS layers illuminated by a normally incident plane wave. Parameters in the title of the graph are described in Fig. 4.

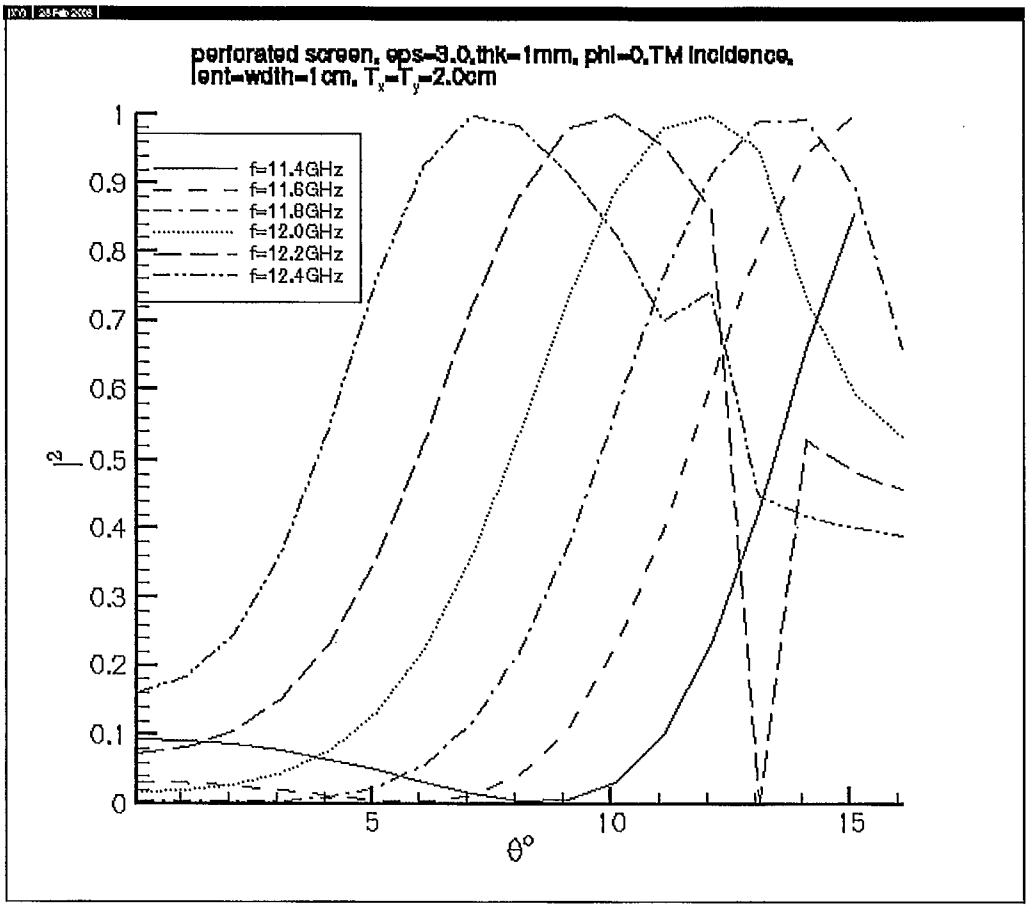

Fig. 9a- Angular sensitivity of a typical perforated screen. The parameters in the title of the plot are described in Fig. 7.

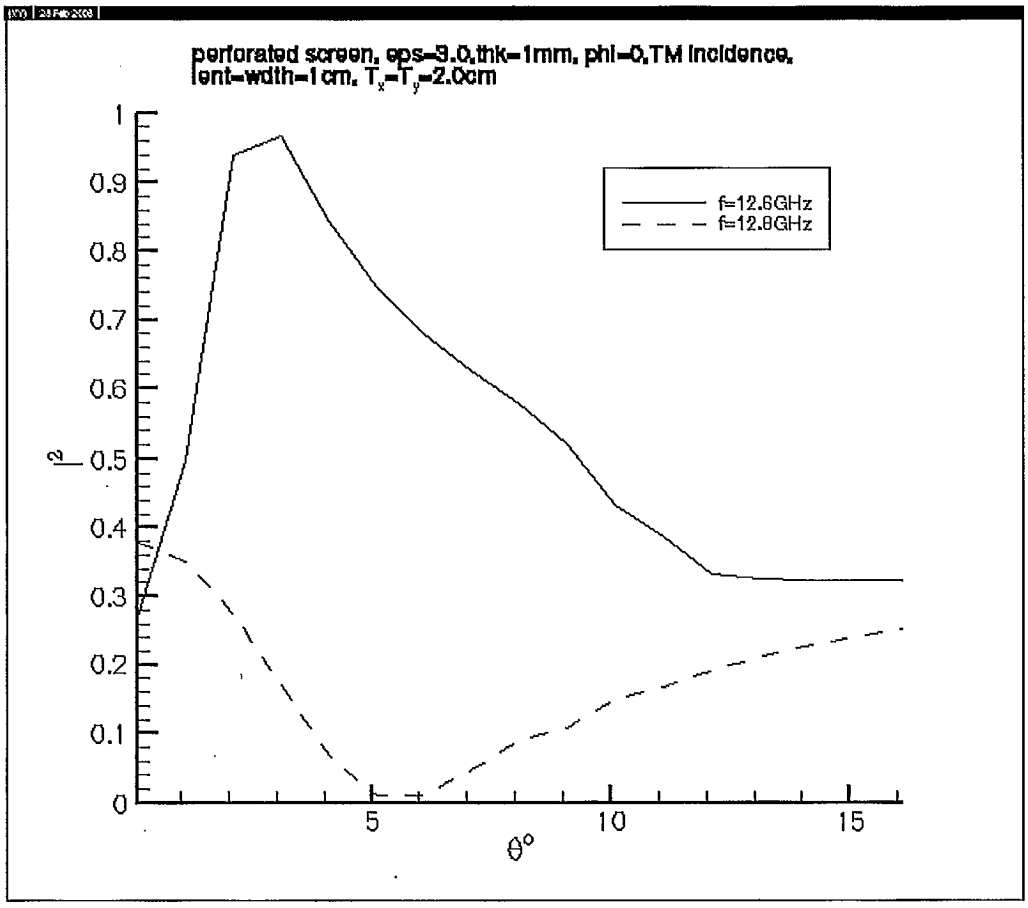

Fig. 9b- Angular sensitivity of a typical perforated screen. The parameters in the title of the plot are described in Fig. 7.

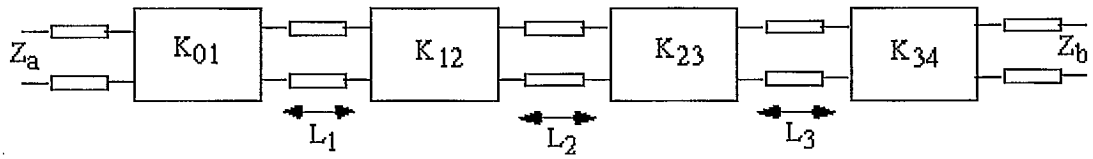

Fig. 10- Block diagram of a Chebishev filter. "K" parameters represent impedance inversion ratios and "L" is resonant lengths of the lines between two consecutive impedance inversion blocks.

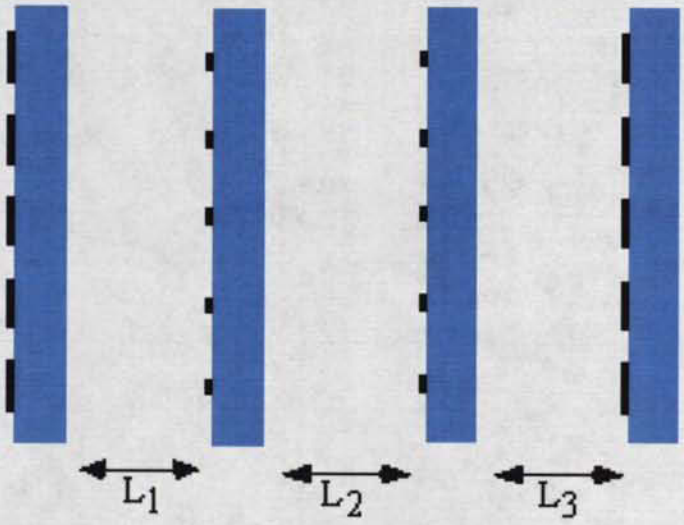

Fig. 11- An FSS implementation of the block diagram shown in Fig. 10.

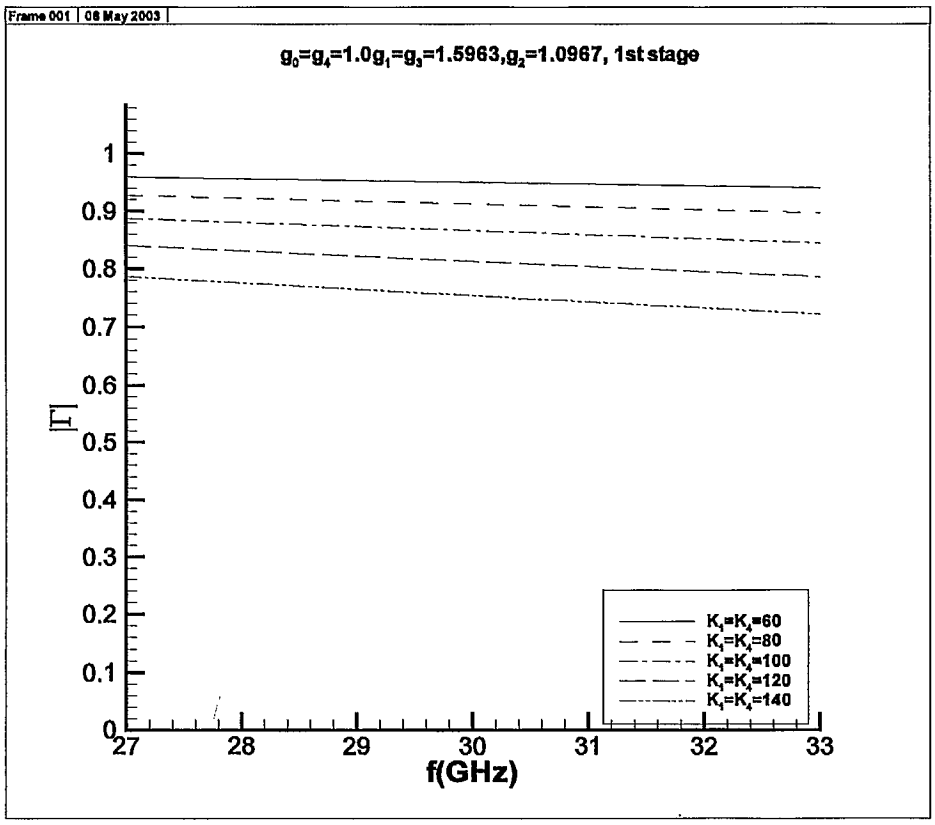

Fig. 12- Frequency response of the reflection coefficient of a single two port stage for different inversion parameters.

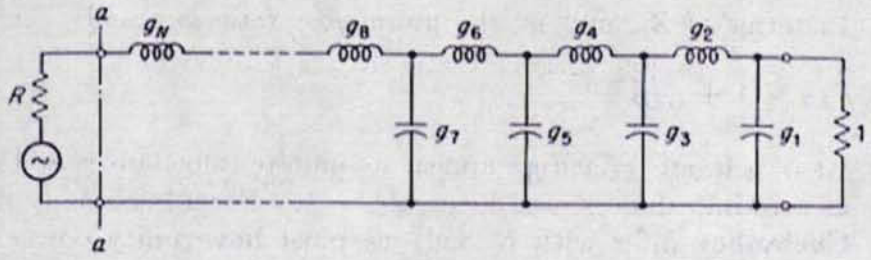

Fig. 13- The circuit representation of the filter from [Collin].

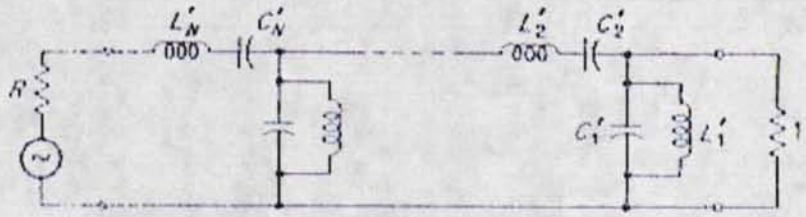

(a)

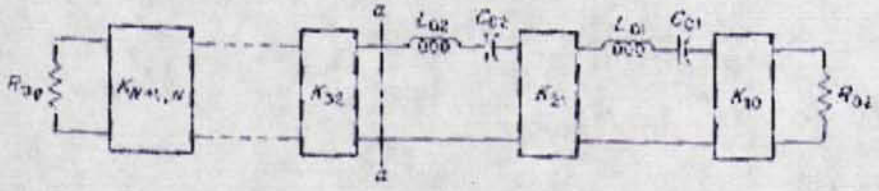

(b)

Fig. 14- Band pass filter:
(a) composed of parallel and series resonant circuits
(b) the parallel resonant circuits have been replaced by impedance inverters

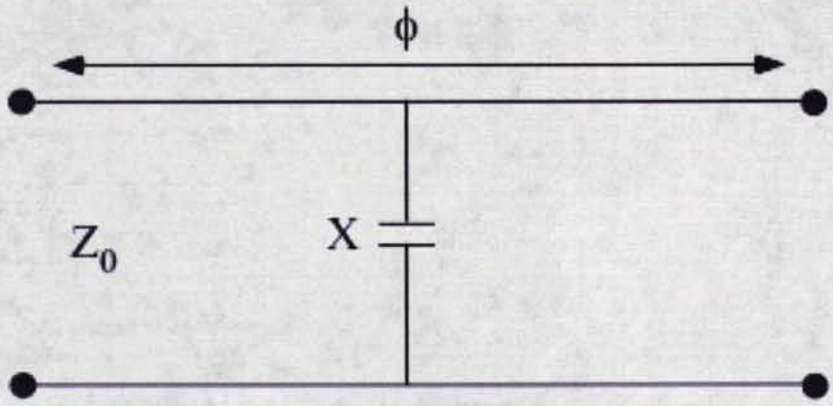

Fig. 15- One of the many circuit realizations of an impedance inverter [Mathai]

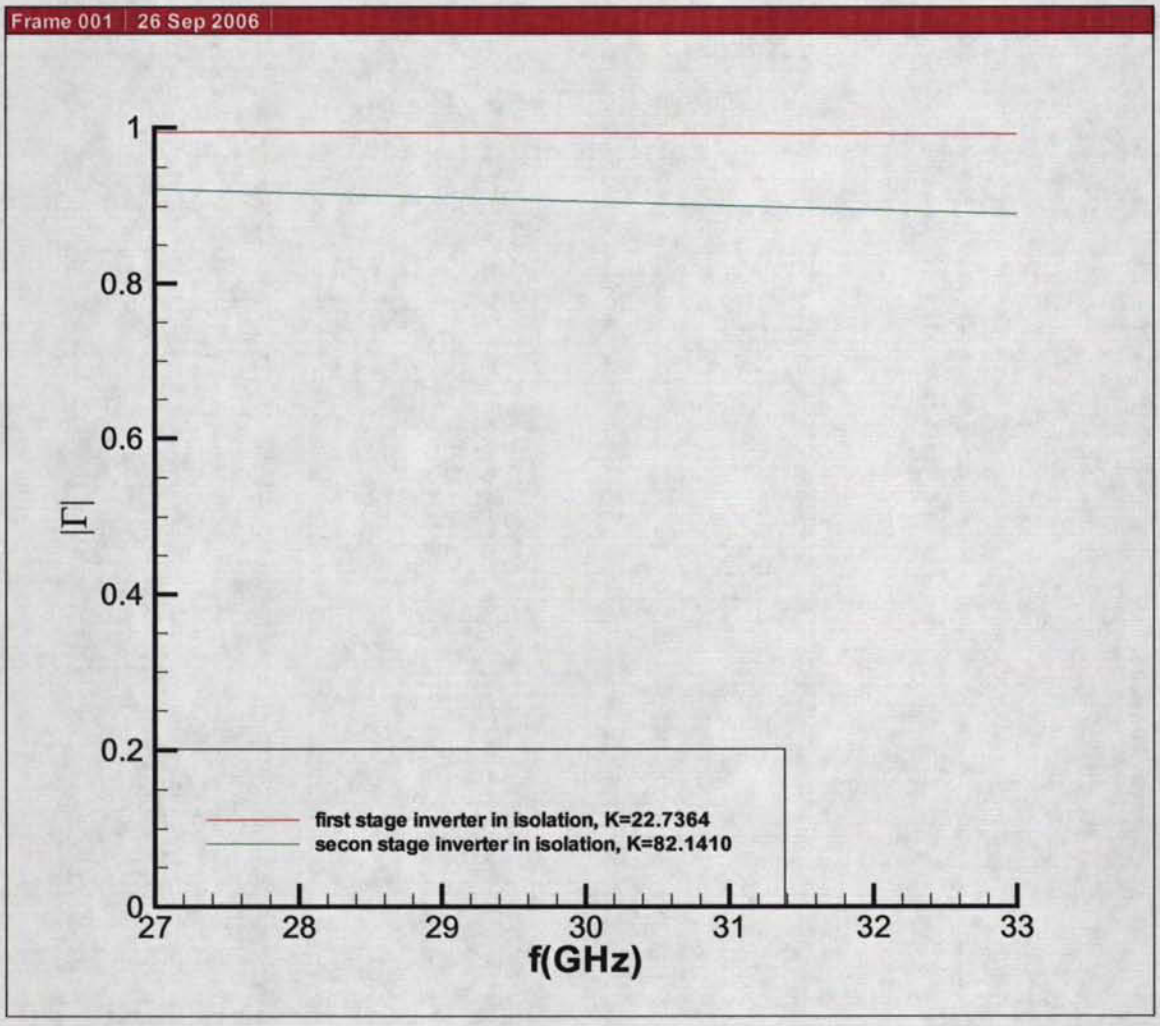

Fig. 16- Frequency response of the first two stages of the filter.

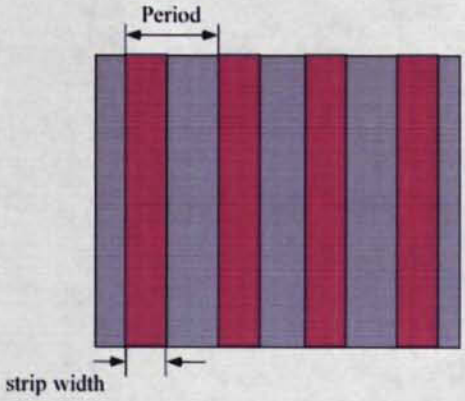

(a)

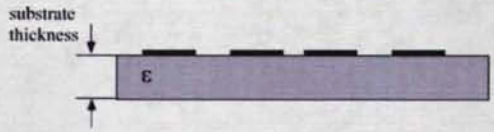

(b)

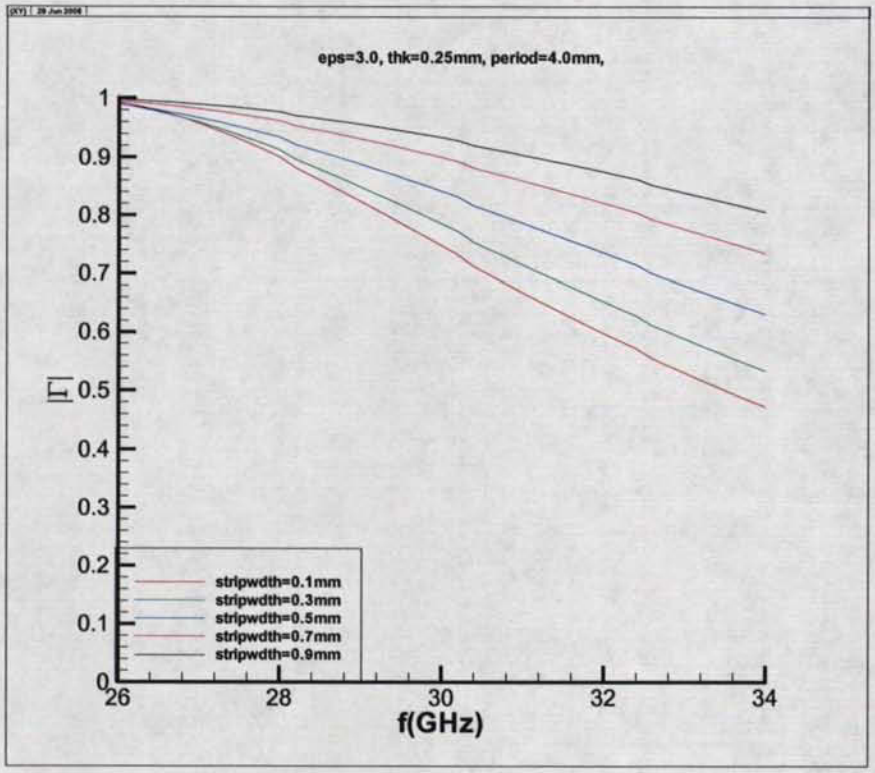

(c)

Fig. 17-
a) Top view of strip grating
b) Side view of strip grating
c) HFSS simulation of strip gratings for different strip widths.

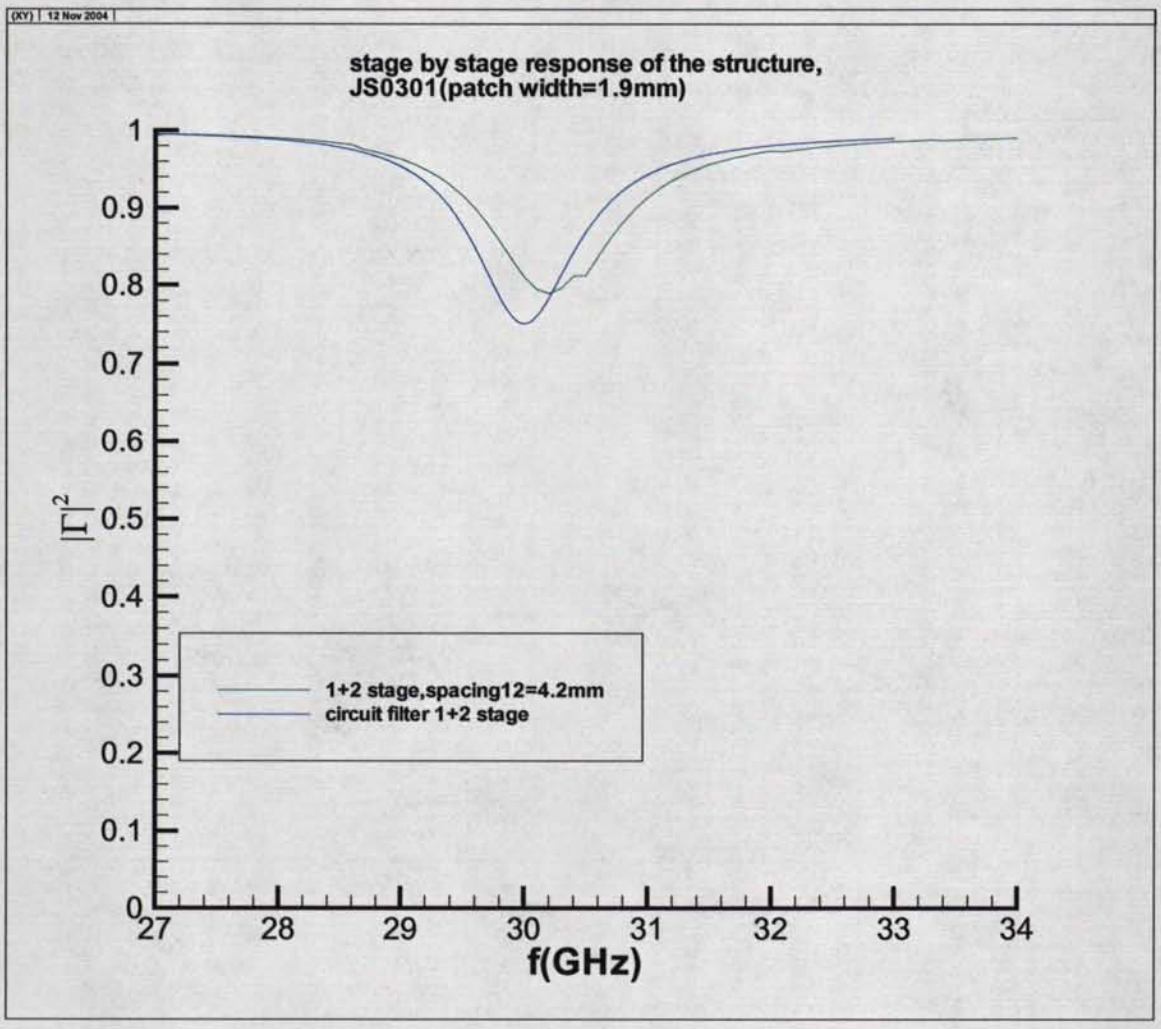

Fig. 18- Frequency characteristics of the two stages of the Chebishev filter composed of FSS layers and the first two stages of the ideal Chebishev filter that utilizes the reflective characteristics of each FSS building block as input.

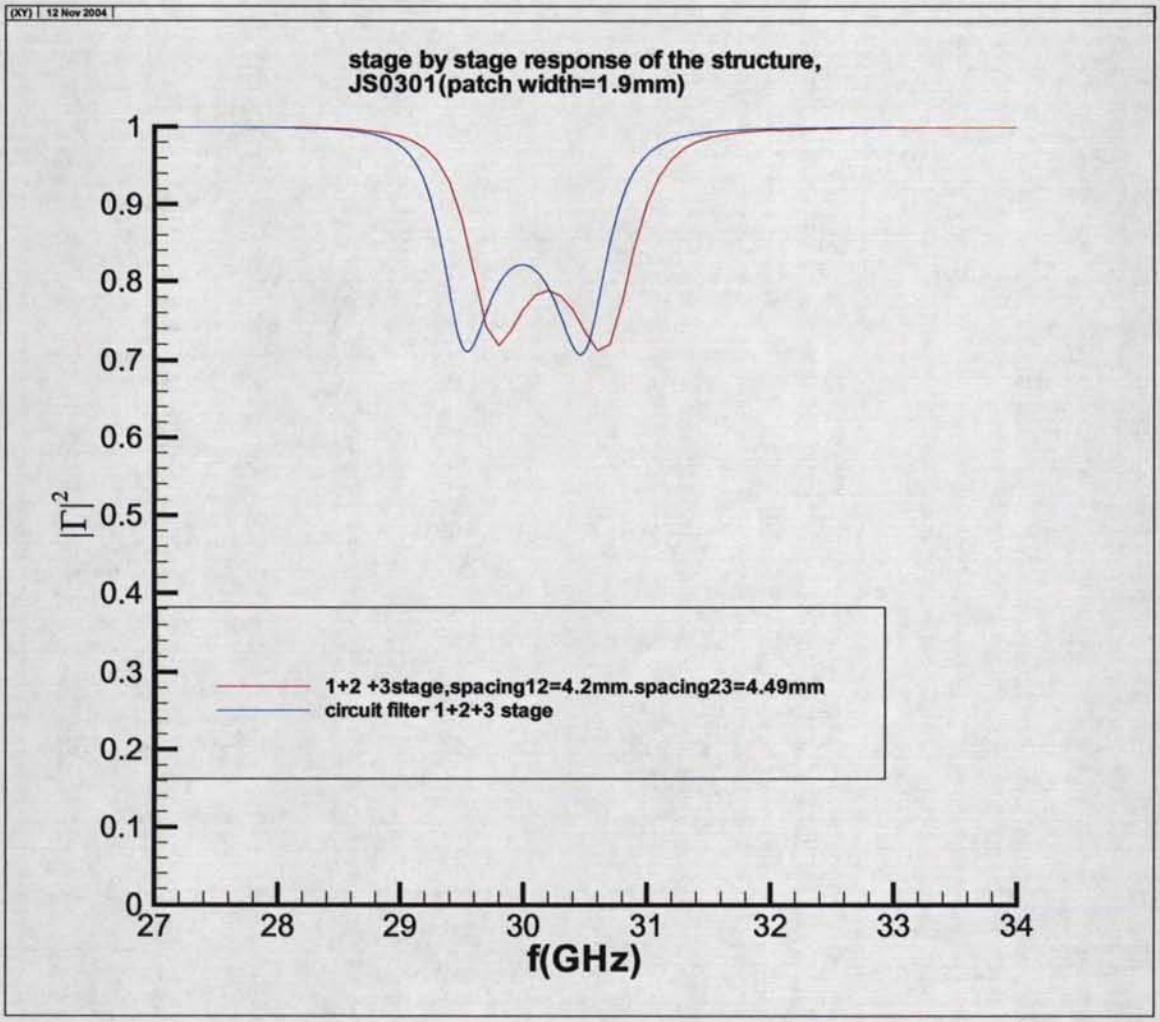

Fig. 19- Frequency characteristics of the three stages of the Chebishev filter composed of FSS layers and the first three stages of the ideal Chebishev filter that utilizes the reflective characteristics of each FSS building block as input.

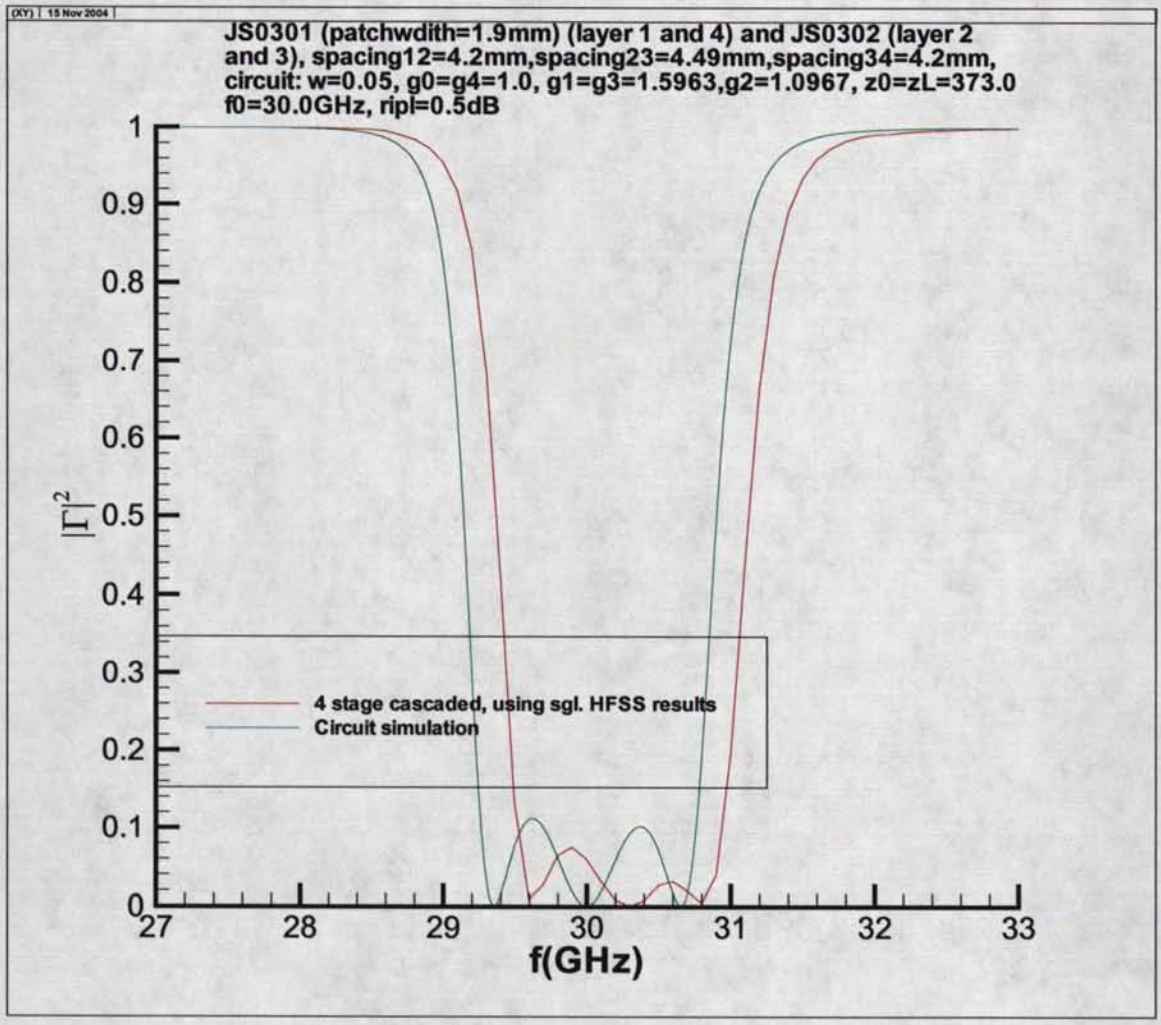

Fig. 20- Frequency characteristics of the four stages of the Chebishev filter composed of FSS layers and the four stages of the ideal Chebishev filter that utilizes the reflective characteristics of each FSS building block as input.

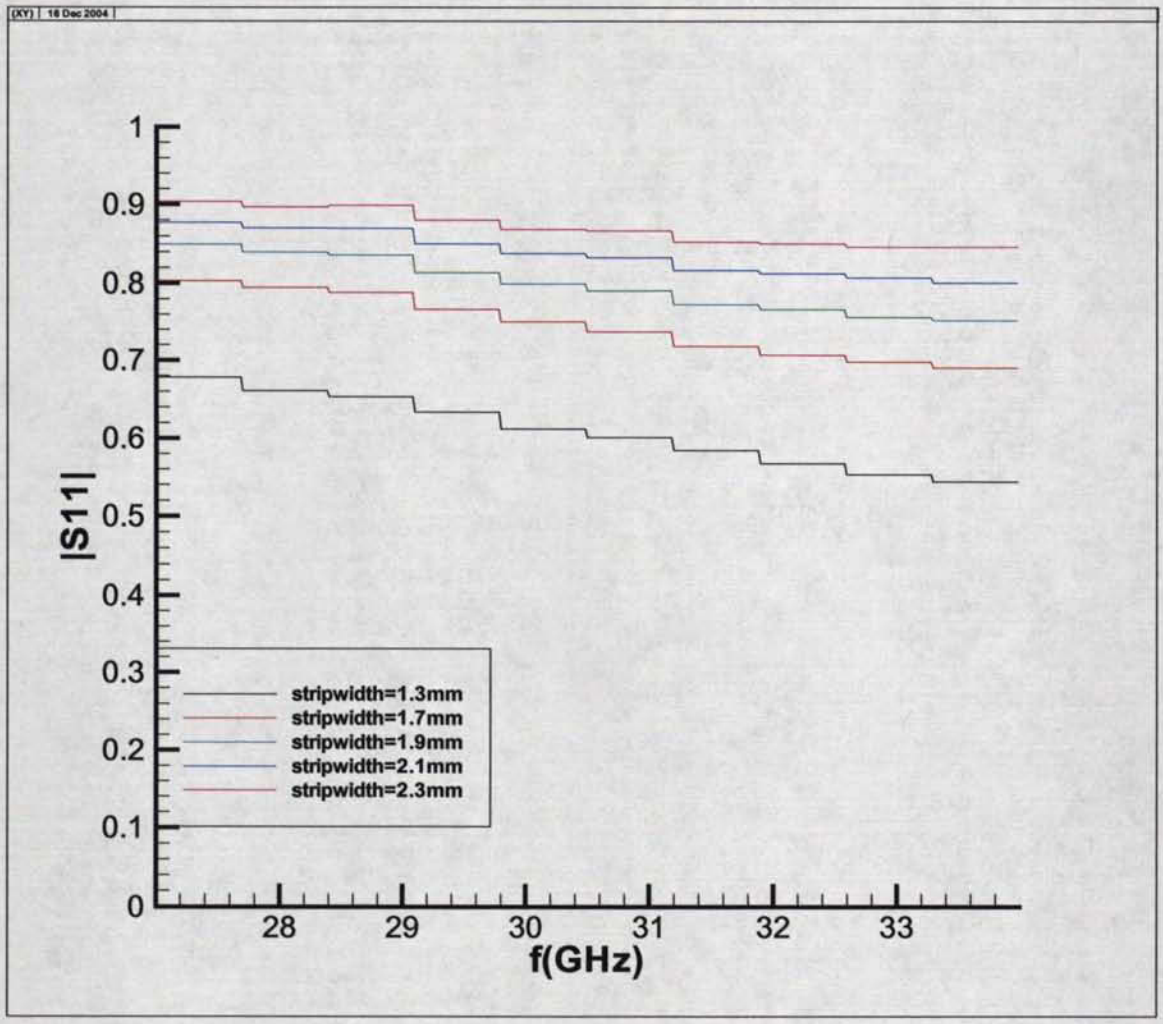

Fig. 21- Measurement of strip gratings with different strip-width:
ε=3.0, substrate thickness=0.25mm, and period=4.0mm.

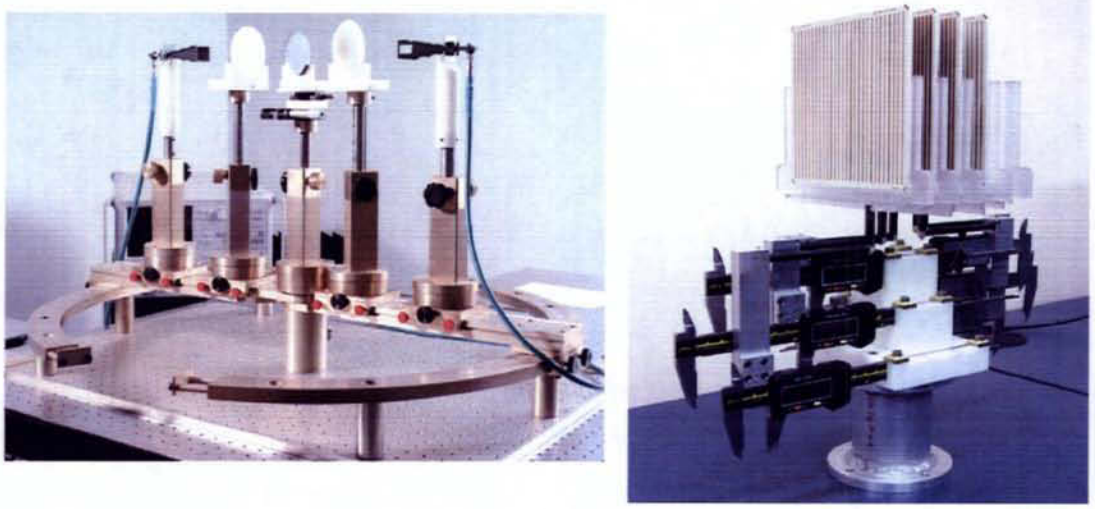

(a) (b)

Fig. 22-

a) Quasi-optical measurement setup the cascaded filter structure was installed on the middle stand.
b) Four layer Chebishev filter composed of FSS layers.

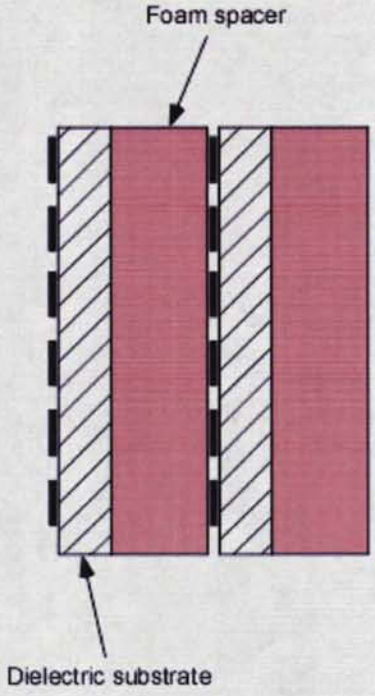

Fig. 23- Configuration of the Fabry-Perot resonator that was used in the simulation and measurement.

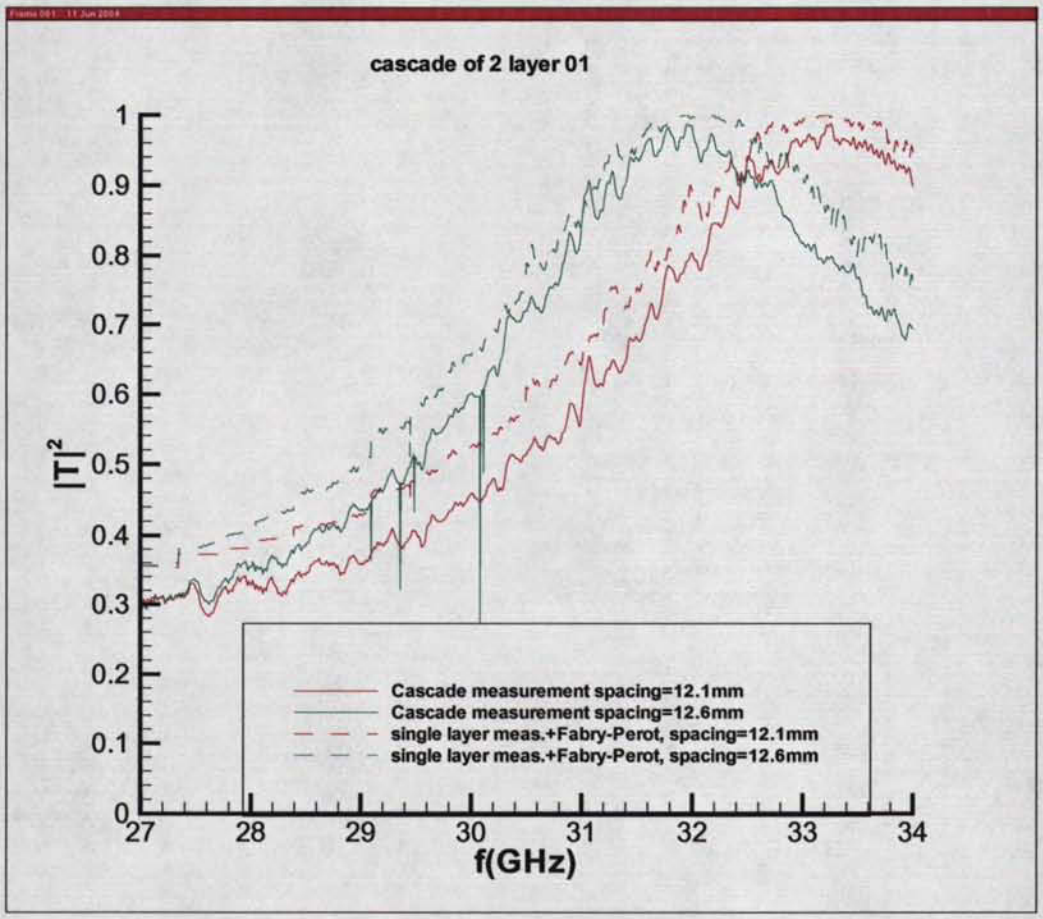

Fig. 24- Measurement for different Fabry-Perot resonators are compared the results of the cascade routine which used single layer measurements as the input to calculate the frequency response of the whole assembly of two layer structure.

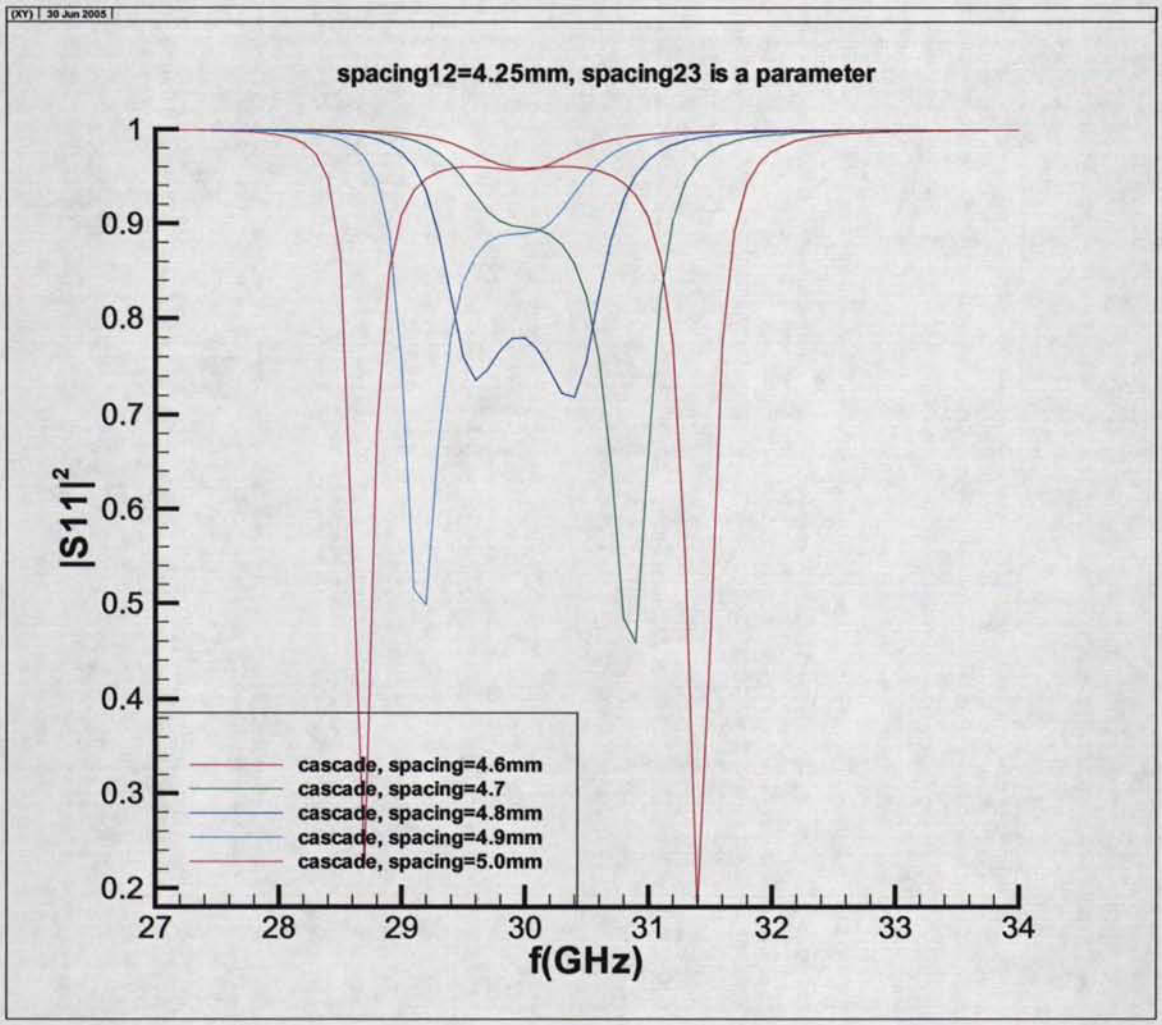

Fig. 25- Frequency response of the cascade of the first three stages for different separations between layers 2 and 3. The separation between layers 1 and 2 was set at 4.25mm.

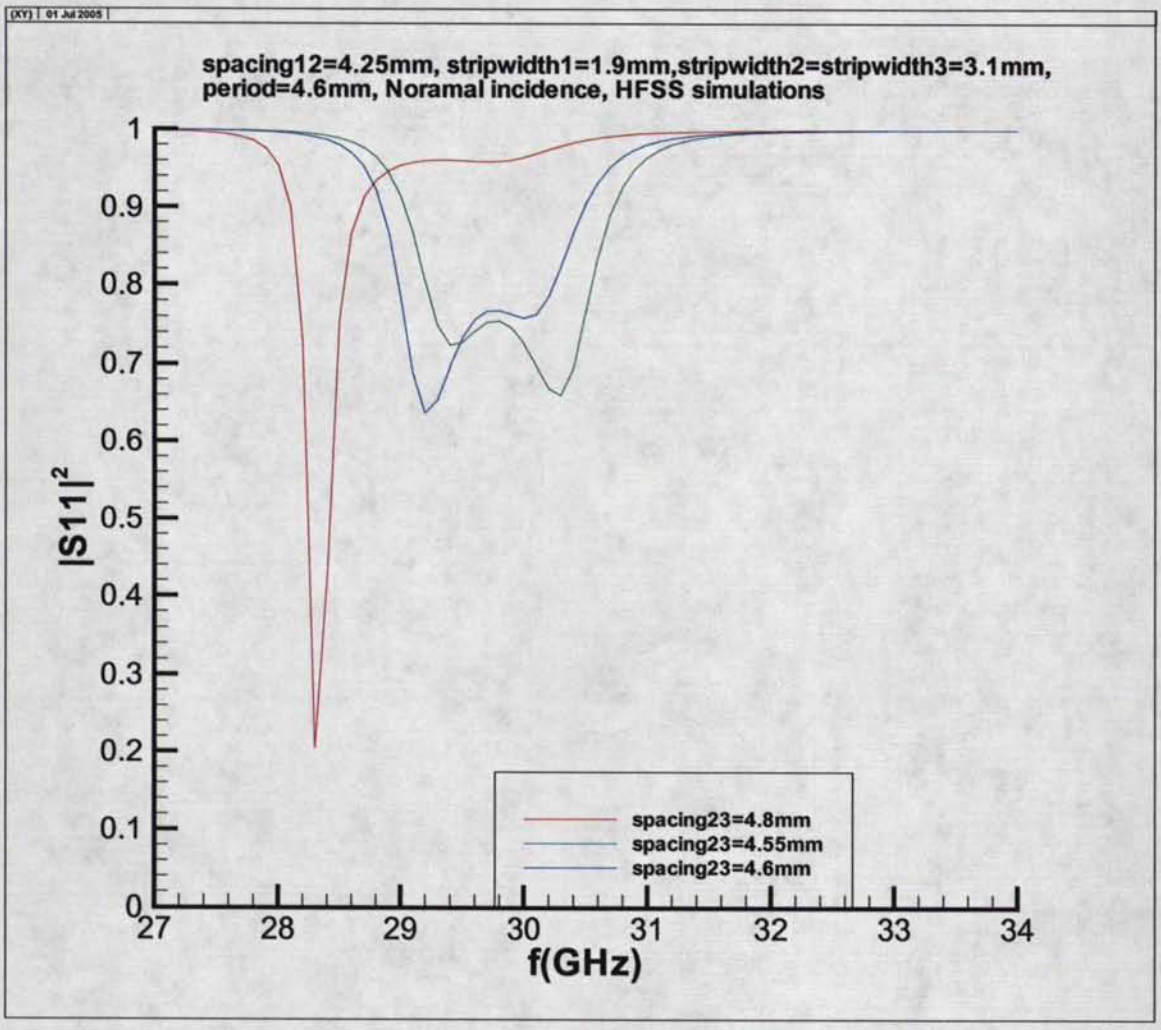

Fig.26- HFSS simulation for small changes in the separation of layers 2 and 3.

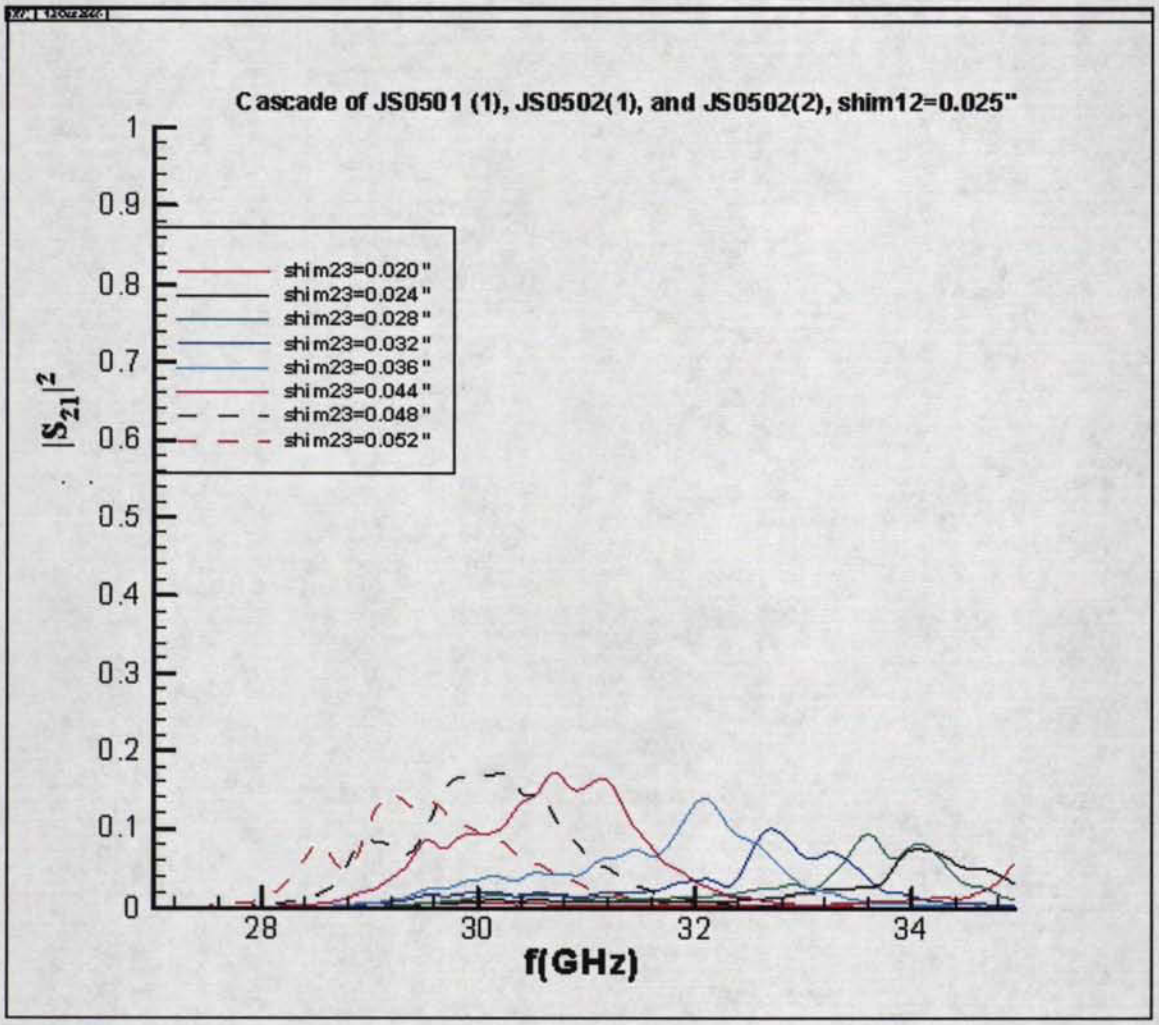

Fig. 27- Measurement of the frequency response of the three-stage structure as the spacing between layers 2 and 3 are changed.

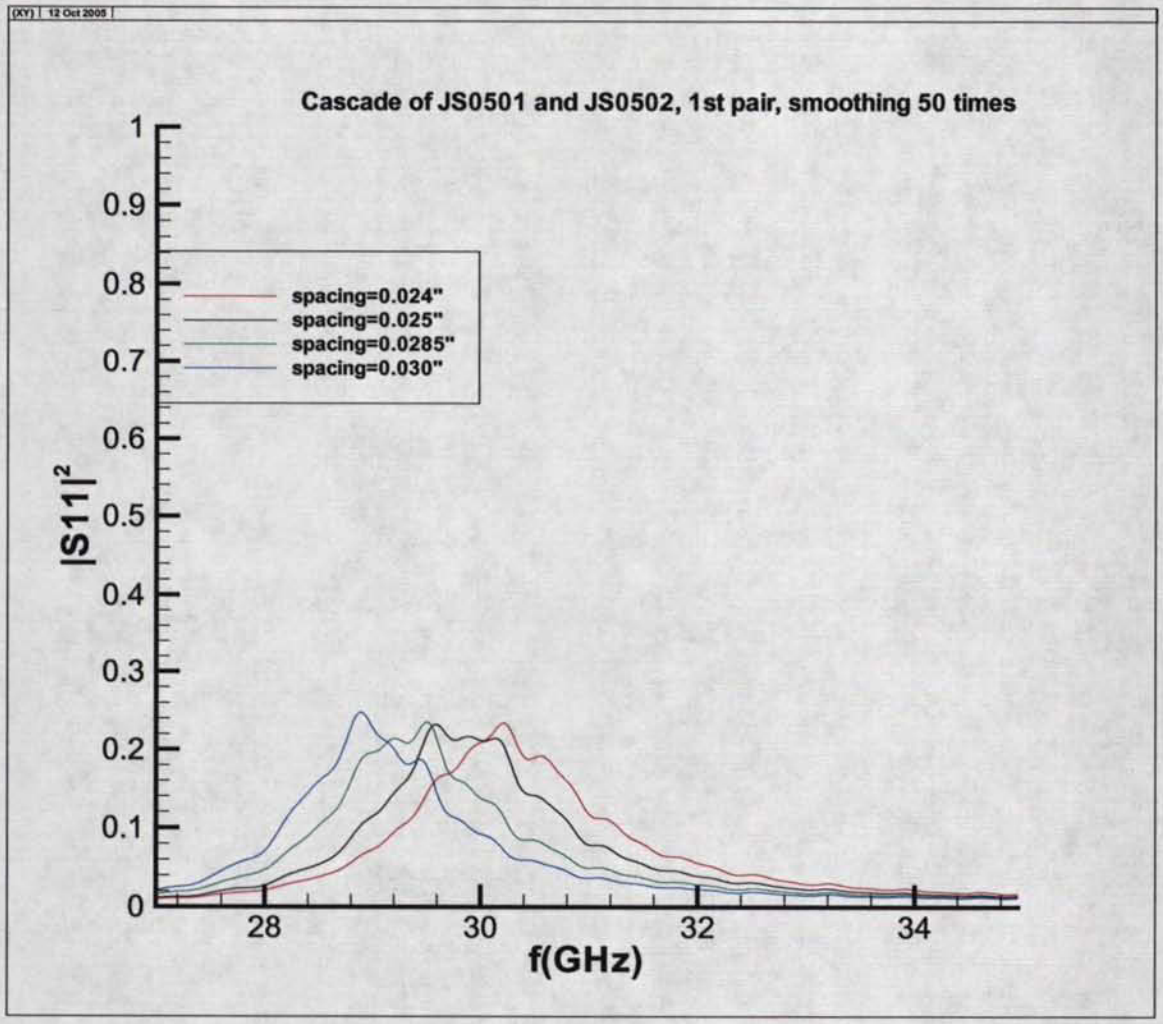

Fig. 28- Frequency response of the two-stage filter as the spacing between layers 1 and 2 was modified by inserting metallic shims between them.

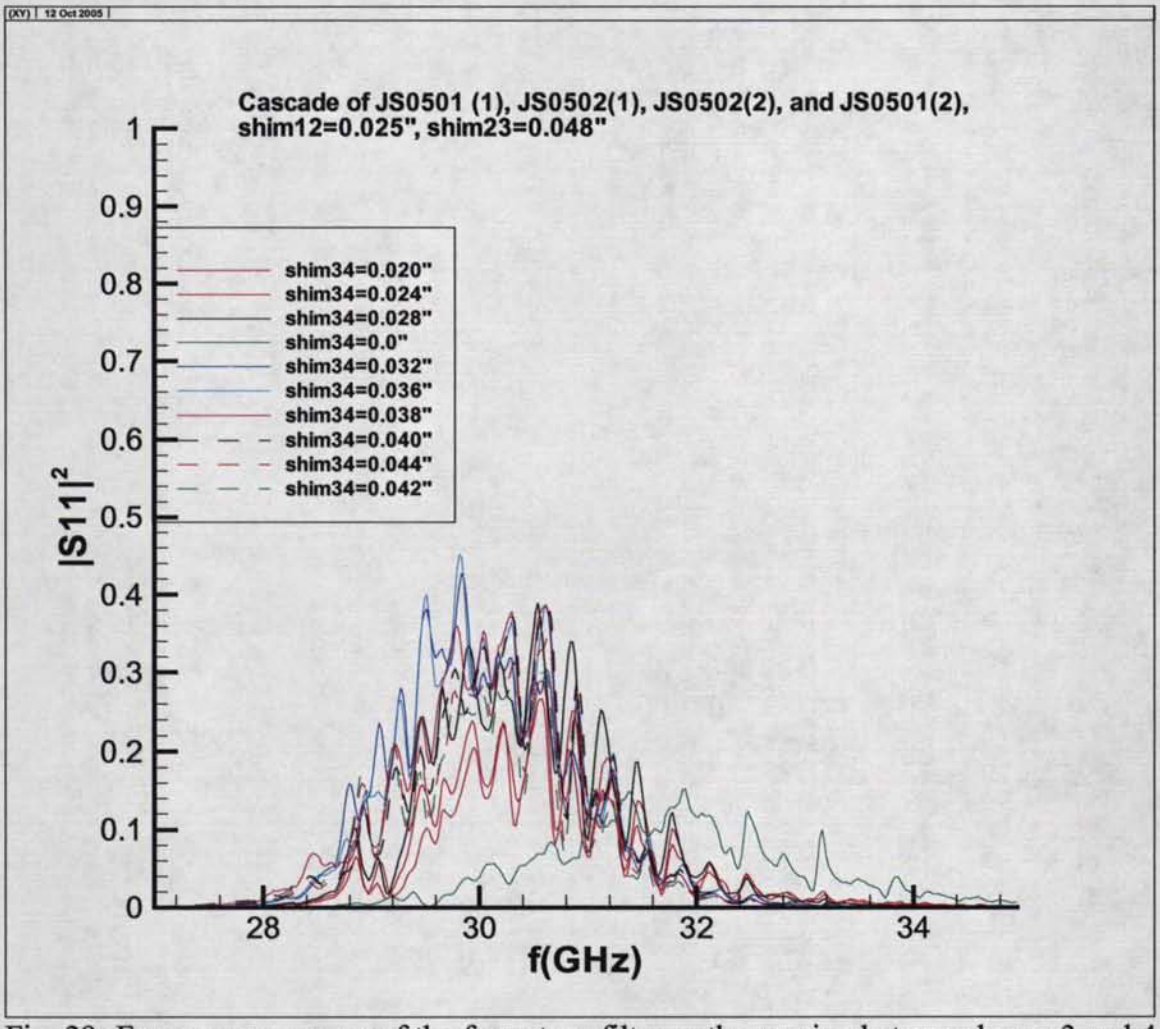

Fig. 29- Frequency response of the four-stage filter as the spacing between layers 3 and 4 was modified by inserting metallic shims between them.

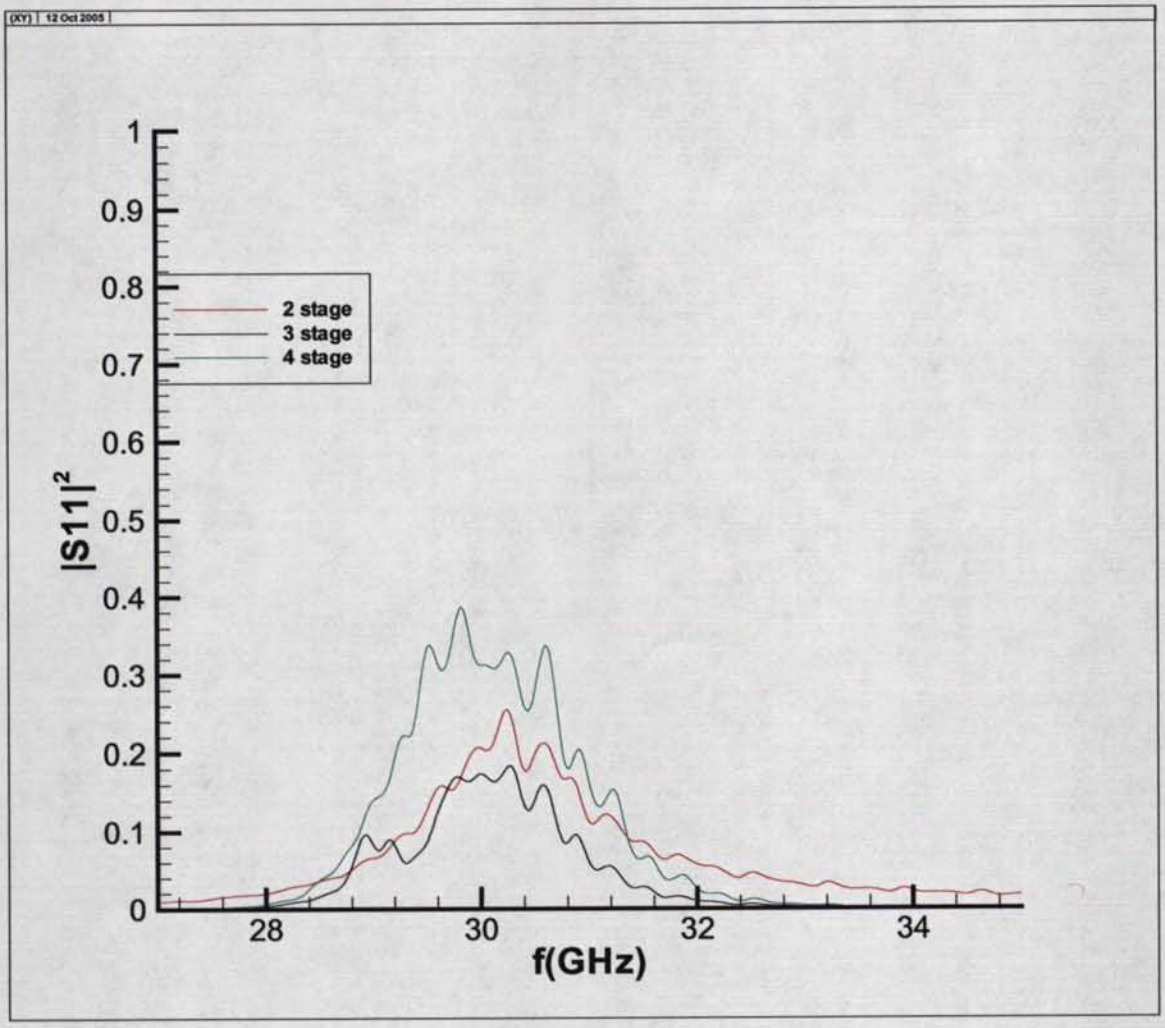

Fig. 30- Frequency response of the filter for optimal separation between the constituent layers.

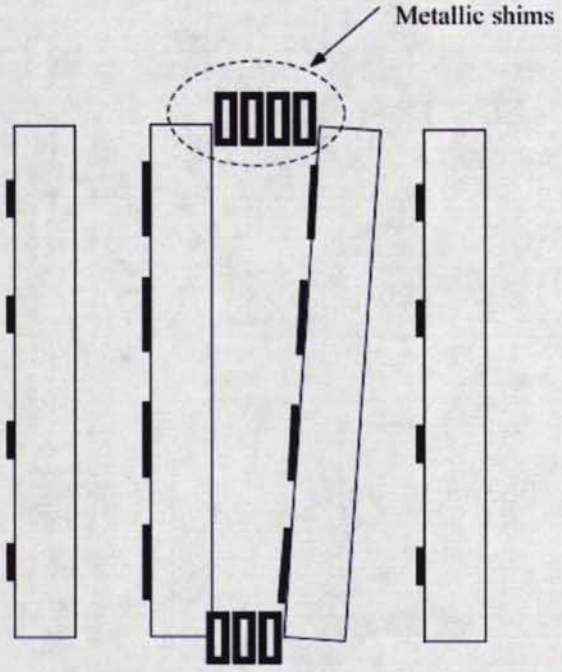

(a)

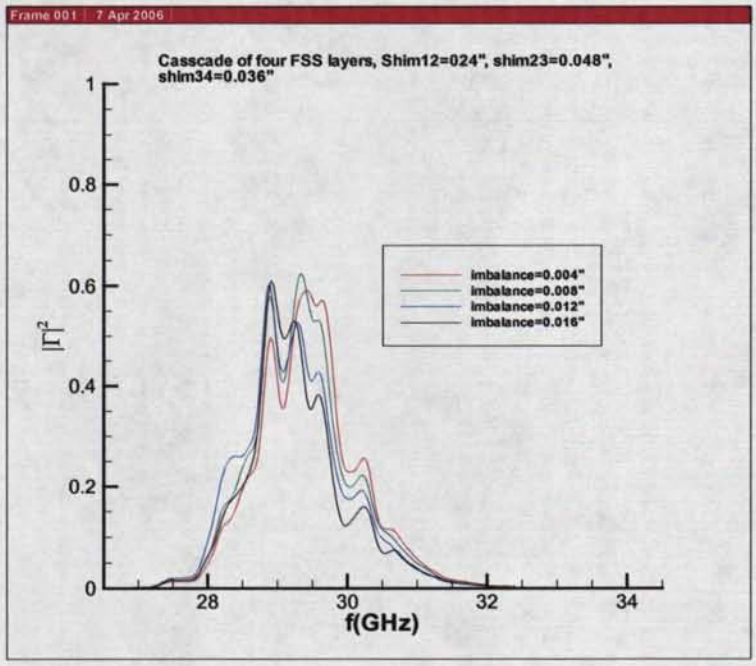

(b)

Fig. 31- Frequency response as shims are inserted between layers 2 and 3:

a) The shims are inserted to raise the separation between two layers only on one side.

b) The resulting frequency response.